Physica Scripta

Physics of ultracold Fermi gases revealed by spectroscopies

OPEN ACCESS
IOP Publishing | Royal Swedish Academy of Sciences Physica Scripta
Phys. Scr. 91 (2016) 043006 (19pp) doi:10.1088/0031-8949/91/4/043006

Invited Comment

Physics of ultracold Fermi gases revealed by spectroscopies

Päivi Törmä

COMP Centre of Excellence, Department of Applied Physics, Aalto University, FI-00076 Aalto, Finland

E-mail: paivi.torma@aalto.fi

Received 10 November 2015, revised 5 February 2016
Accepted for publication 10 February 2016
Published 22 March 2016

Abstract

This article provides a brief review of how various spectroscopies have been used to investitage many-body quantum phenomena in the context of ultracold Fermi gases. In particular, work done with RF spectroscopy, Bragg spectroscopy and lattice modulation spectroscopy is considered. The theoretical basis of these spectroscopies, namely linear response theory in the many-body quantum physics context is briefly presented. Experiments related to the BCS–BEC crossover, imbalanced Fermi gases, polarons, possible pseudogap and Fermi liquid behaviour and measuring the contact are discussed. Remaining open problems and goals in the field are sketched from the perspective how spectroscopies could contribute.

Keywords: ultracold quantum gases, ultracold Fermi gases, RF spectroscopy, Bragg spectroscopy, lattice modulation spectroscopy, BCS–BEC crossover, imbalanced Fermi gases

(Some figures may appear in colour only in the online journal)

1. Introduction

One remarkable use of light, or radiation in general, is spectroscopy. Throughout the history of science, it has helped the humankind to discover, analyse, diagnose and understand. Here I discuss spectroscopies in one specific important context, namely ultracold Fermi gases. Ultracold Fermi gases have already enabled remarkable achievements, such as establishing experimentally the existence of the Bardeen–Cooper–Schrieffer (BCS)–Bose–Einstein condensation (BEC) crossover, i.e. crossover between BCS type superfluidity and BEC. In the year of light, 2015, it is timely to discuss how spectroscopies have contributed to these successes and how they could be used for solving remaining and new problems. It is timely also because the year 2015 is the tenth anniversary of fermionic superfluidity in ultracold gases.

The aim here is to briefly review some of the most important topics explored by spectroscopies in the context of ultracold Fermi gases. I have already written a book chapter on the theory of spectroscopies in ultracold gases [1]; there, the focus was on detailed explanation of the physics of the spectroscopies themselves, from the quantum many-body perspective, while the research done using them was hardly reviewed at all. Here the focus is exactly the opposite: the book chapter and this article are thus complementary and together form a substantial study material for anybody who wishes to start understanding the topic in depth. For a researcher who begins to use a certain method in lab or in calculations, it shoud be useful both to understand the theoretical basis as well as get inspiration from research problems the method has already been applied to. This gives the motivation for me to write both the book chapter and this article. In addition, although the focus on spectroscopies makes it somewhat incomplete and biased, this article serves also as a quick overview of the main physics explored with ultracold Fermi gases within the last then years.

There are already several excellent review articles which discuss physics of ultracold Fermi gases; here a few

comments about the overlap and the differences comparted to this article (and my related book chapter [1]). Two famous reviews appeared in 2008, on many-body physics with ultracold gases by Bloch, Dalibard and Zwerger [2], and on theory of ultracold atomic Fermi gases by Giorgini, Pitaevskii and Stringari [3]. Due to the vast scope of these reviews, the discussion on physics of ultracold Fermi gases revealed by spectroscopies is a bit more brief than presented here and in [1]. This is the case also with some more recent reviews such as the one by Randeria and Taylor 2014 [4]. A classic book chapter on ultracold Fermi gases was written by Zwierlein and Ketterle in 2008 [5]. Therein, presentation of spectroscopies and physics revealed by them is very thorough, however, only developments until mid 2008 are discussed. Reference [5] has a substantial overlap with this article concerning the years 2003–2007, but for the sake of completeness, I wish to repeat the discussions of the early experiments. There is also a review focusing on the possibility of a pseudogap in ultracold Fermi gases by Chen, Levin and coworkers from 2009 [6] which has overlap with related discussions here. Since 2009, reviews on specific topics within the research of ultracold Fermi gases have appeared: on density imbalanced gases by Sheehy and Radzihovsky [7, 8], by Chevy and Mora [9], and by Gubbels and Stoof [10], on lattice physics by Georges and Giamarchi [11], on polarons by Massignan, Zaccati and Bruun [12], and on 2D Fermi gases by Levinsen and Parish [13]. Some of these discuss particular spectroscopy experiments related to the topic of this article, and I will cite these in the sections below. This article presents briefly all major ultracold Fermi gas physics achievements where spectroscopies played a role during 2003–2015; it is therefore suited for a reader who wishes to get a quick glance through all the doors that spectroscopies have opened during the last decade.

I will first present in sections 2 and 3 the theoretical formalism of the three spectroscopies that are in focus: RF spectroscopy (see figure 1), Bragg spectroscopy, and lattice modulation spectroscopy. Sections 2 and 3, and to some extent section 4, consitute a summary of the theoretical description of spectroscopies given my book chapter [1]. These sections provide a selection of the main steps in the theoretical description for those readers that want an overall picture of the theory and enough background information to understand the rest of the article. In contrast, my lengthy book chapter [1] serves a different purpose by providing details and in-depth description for those who, for instance, wish to use the theoretical formalism in their work. I then proceed to describe the physics: how spectroscopies contributed to understanding issues such as BCS-type pairing and molecule formation, BCS–BEC crossover, the pairing gap, imbalanced Fermi gases and quasiparticle spectroscopy, the Mott-insulator phase for fermions in lattices, the contact, and the pseudogap versus Fermi liquid nature of the normal state. Future expected uses of spectroscopies, for instance in probing the Fulde–Ferrel–Larkin–Ovchinnikov (FFLO) state, are outlined as well.

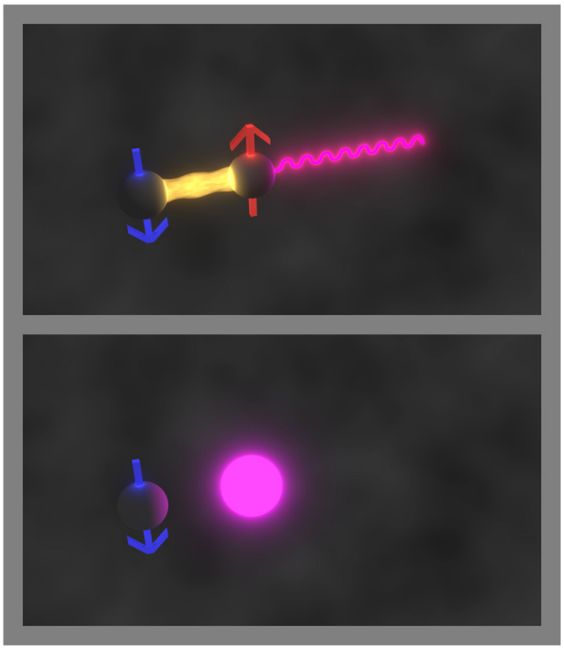

Figure 1. Schematic of probing pairing by spectroscopies. The two fermions of different species (different pseudospins) correspond to either different internal states of an atom, or two different atomic species or isotopes. They form Cooper pairs or molecules due Feshbach-resonance enhanced interparticle interactions (yellow). The probing field (the pink photon) transfers one of the species to a third one (another internal state, depicted by the pink sphere). The pair is broken. The energy needed for this process is shifted, due to the pairing energy, from the energy difference between the two internal states. This leads to spectral shifts that can be related to the properties of the molecule or the many-body state. Picture by Antti Paraoanu and reproduced with permission.

2. The theoretical basis of the spectroscopies

Spectroscopies are usually based on the principles of linear response. It is assumed that the probing field (light or other electromagnetic field) is a weak perturbation to the system, and the response thus represents basically properties of the probed system of interest, not the dynamics of the combined entity including the field and the system, see figure 1. Linear response theory often leads to the Fermi's golden rule, but in case of interacting many-body systems, one should be cautious to straighforwardly apply a simple Fermi golden rule formula. It is better to start from general linear response theory for many-body states, and carefully check which types of approximations are justified in the particular case of study. A detailed theoretical description suited for guiding such analysis is given in my book chapter [1]. Here I will now present the theoretical basis of ultracold gas spectroscopies only briefly; for subtle details and further information please see [1]. I will first discuss a typical system Hamiltonian for an ultracold Fermi gas, then present the first and second order linear response formulas in a general form, and finally discuss

how they apply to RF, Bragg and lattice modulation spectroscopies.

2.1. The system and its Hamiltonian

We are now interested in systems with several species of fermionic particles, possibly interacting with each other, and probed by a field. The fermions correspond to field operators $\hat{\psi}_\sigma(\mathbf{r})$ where σ denotes the distinguishable species of particles, that is, (pseudo)spins. The pseudospins can in general be for instance atoms in different internal states or even different atomic or molecular species. Let us denote the mass, internal state energy and the external (trapping) potential for the different species by m_σ, E_σ and $V_{T,\sigma}(\mathbf{r})$, respectively. In addition, the particles may be interacting via a two-particle potential $V_{\alpha\beta}(\mathbf{r}, \mathbf{r}')$. To describe spectroscopic response to a field, we furthermore introduce the field $\Omega_{\gamma\delta}(\mathbf{r}, t)$ which couples two species. Note that in order for two species to be coupled by a field, they need to be internal states of the same atom (i.e. not two species that are two different atoms). The Rabi coupling has the usual definition $\Omega_{\gamma\delta}(\mathbf{r}, t) = -\mathbf{d}_{\gamma\delta}\cdot\mathcal{E}(\mathbf{r}, t)/\hbar$. Here $\mathbf{d}_{\gamma\delta}$ is the transition dipole moment between the two internal states and $\mathcal{E}(\mathbf{r}, t)$ is the electric field amplitude. The Hamiltonian of such a system expressed in the second quantized field theoretical formalism is

$$\begin{aligned}\hat{H}_C = &\int \mathrm{d}^3 r \sum_\sigma \hat{\psi}_\sigma^\dagger(\mathbf{r})\left(-\frac{\hbar^2\nabla^2}{2m_\sigma} + E_\sigma + V_{T,\sigma}(\mathbf{r})\right)\hat{\psi}_\sigma(\mathbf{r})\\ &+ \frac{1}{2}\sum_{\alpha,\beta}\int \mathrm{d}^3 r \int \mathrm{d}^3 r' V_{\alpha\beta}(\mathbf{r}, \mathbf{r}')\hat{\psi}_\alpha^\dagger(\mathbf{r})\hat{\psi}_\beta^\dagger(\mathbf{r}')\\ &\times \hat{\psi}_\beta(\mathbf{r}')\hat{\psi}_\alpha(\mathbf{r})\\ &+ \sum_{\gamma,\delta}\int \mathrm{d}^3 r\,[\hbar\Omega_{\gamma\delta}(\mathbf{r}, t)\hat{\psi}_\gamma^\dagger(\mathbf{r})\hat{\psi}_\delta(\mathbf{r}) + \text{h.c.}].\end{aligned} \tag{1}$$

Note that the sets of species corresponding to the indices α, β and γ, δ are not necessarily the same. There can be, for instance, interacting species that do not interact with any fields. And the field may transfer one species to another one that does not interact with the rest of the species. This Hamiltonian describes the full many-body quantum physics of the particles and the interaction with the field, albeit the field is assumed to be classical. The Hamiltonian is written in the canonical ensemble (C for canonical in $\hat{H}_C$). Correspondingly, the chemical potentials μ_σ are not part of the Hamiltonian. This must be the case because the Hamiltonian (1) (its last line) does not conserve particle number.

To proceed with the calculations, it is convenient to divide the Hamiltonian (1) so that $\hat{H}_L'(t)$ refers to the last line and the rest of the Hamiltonian is labeled by $\hat{H}_{0C}$.

2.2. Linear response for many-body quantum states

We now proceed to give the linear response formulas that describe the spectroscopic response. For that purpose, we make the Hamiltonian (1) slightly more specific.

Let us consider only one field that couples only two species (internal states). In the Hamiltonian (1) the last line then will not have summation over species indices but only two of them, say e and g. The state g does not need to be the ground state but is chosen to be lower in energy than the state e. In the rest of the Hamiltonian, which describes a complicated many-body system, also other species and indices than e and g may also appear. The Hamiltonian becomes

$$\begin{aligned}\hat{H}_C = &\int \mathrm{d}^3 r \sum_\sigma \hat{\psi}_\sigma^\dagger(\mathbf{r})\left(-\frac{\hbar^2\nabla^2}{2m_\sigma} + E_\sigma + V_{T,\sigma}(\mathbf{r})\right)\hat{\psi}_\sigma(\mathbf{r})\\ &+ \frac{1}{2}\sum_{\alpha,\beta}\int \mathrm{d}^3 r \int \mathrm{d}^3 r' V_{\alpha\beta}(\mathbf{r}, \mathbf{r}')\hat{\psi}_\alpha^\dagger(\mathbf{r})\hat{\psi}_\beta^\dagger(\mathbf{r}')\\ &\times \hat{\psi}_\beta(\mathbf{r}')\hat{\psi}_\alpha(\mathbf{r})\\ &+ \int \mathrm{d}^3 r\,[\hbar\Omega(\mathbf{r}, t)\hat{\psi}_e^\dagger(\mathbf{r})\hat{\psi}_g(\mathbf{r}) + \text{h.c.}].\end{aligned} \tag{2}$$

The response can be calculated in several ways. One option is to monitor the number of particles in, say, state e, namely $\hat{n}_e$. Here we consider, instead, the rate of change in the particle number, $\hat{\dot{n}}_e = \frac{\mathrm{d}}{\mathrm{d}t}(\hat{\psi}_e^\dagger(\mathbf{r})\hat{\psi}_e(\mathbf{r}))$; this is like calculating the transition rate instead of the transition probablility. We made this choice because $\hat{\dot{n}}_e$ is the same as current in electrical transport. Currents are conveniently given by the so-called Kubo formulas, described, for instance, in [14] section 3.8. Note, however, that we will actually use $\hat{n}$ when describing the Bragg spectroscopy response.

Let us continue by a reminder of some basic concepts of linear response theory in general. To obtain the expectation value for any observable (operator) $\hat{O}$, one can make a perturbation expansion with respect to the perturbation part of the Hamiltonian $\hat{H}_L'$. In our case $\hat{H}_L'$ equals the last line of (2) while the remaining terms of the Hamiltonian are denoted by $\hat{H}_{0C}$. In the interaction picture one has

$$\hat{\psi}_{\sigma C}^\dagger(\mathbf{r}, t) = \mathrm{e}^{\mathrm{i}\hat{H}_{0C}t/\hbar}\hat{\psi}_\sigma^\dagger(\mathbf{r})\mathrm{e}^{-\mathrm{i}\hat{H}_{0C}t/\hbar}, \tag{3}$$

$$\hat{H}_{LC}(\mathbf{r}, t) = \mathrm{e}^{\mathrm{i}\hat{H}_{0C}t/\hbar}\hat{H}_L'(\mathbf{r}, t)\mathrm{e}^{-\mathrm{i}\hat{H}_{0C}t/\hbar} \equiv \hat{H}_L(t). \tag{4}$$

The time-evolution of the state $|\Psi\rangle$ becomes

$$|\Psi(t)\rangle = U(t, t_0)|\Psi(t_0)\rangle, \tag{5}$$

where

$$\begin{aligned}U(t, t_0) &= T\exp\left(-\frac{\mathrm{i}}{\hbar}\int_{t_0}^t \mathrm{d}t'\hat{H}_L(t')\right)\\ &= 1 - \frac{\mathrm{i}}{\hbar}\int_{t_0}^t \mathrm{d}t'\hat{H}_L(t')\\ &\quad - \frac{1}{\hbar^2}\int_{t_0}^t \mathrm{d}t'\int_{t_0}^{t'} \mathrm{d}t''\hat{H}_L(t')\hat{H}_L(t'') + \mathcal{O}(\hat{H}_L^3).\end{aligned} \tag{6}$$

Only the first two terms are of this expasion are considered when calculating the linear response approximation of $\langle\Psi|\hat{O}(\mathbf{r}, t)|\Psi\rangle$. This gives only the constant $\langle\Psi(t_0)|\hat{O}|\Psi(t_0)\rangle$ and terms linear (first order) in $\hat{H}_L$. A quantity that naturally emerges is the first order susceptibility

$$\chi(t, t') = \frac{1}{\mathrm{i}\hbar}\theta(t - t')\langle[\hat{O}(\mathbf{r}, t), \hat{H}_L(t')]\rangle. \tag{7}$$

The result for the expectation value of the operator becomes

$$\begin{aligned}\langle\Psi(t)|\hat{O}(\mathbf{r},\,t)\;|\Psi(t)\rangle_{1\mathrm{st}}&=-\frac{\mathrm{i}}{\hbar}\langle\Psi(t_0)|\int_{t_0}^{t}\mathrm{d}t'\,[\hat{O}(\mathbf{r},\,t),\,\hat{H}_L(t')]|\Psi(t_0)\rangle\\&=-\frac{\mathrm{i}}{\hbar}\int_{t_0}^{t}\mathrm{d}t'\,\langle[\hat{O}(\mathbf{r},\,t),\,\hat{H}_L(t')]\rangle\\&\equiv\int_{t_0}^{\infty}\mathrm{d}t'\chi(t,\,t'),\end{aligned}\tag{8}$$

here the notation $|\rangle = |\Psi(t_0)\rangle$ is used. Putting together terms of second order in $\hat{H}_L$ leads to

$$\begin{aligned}\langle\Psi(t)|\hat{O}(\mathbf{r},\,t)\;|\Psi(t)\rangle_{2\mathrm{nd}}&=-\frac{1}{\hbar^2}\Bigg(\int_{t_0}^{t}\int_{t_0}^{t'}\mathrm{d}t'\mathrm{d}t''\langle\hat{H}_L(t'')\hat{H}_L(t')\hat{O}(\mathbf{r},\,t)\rangle\\&\quad-\int_{t_0}^{t}\int_{t_0}^{t}\mathrm{d}t'\mathrm{d}t''\langle\hat{H}_L(t')\hat{O}(\mathbf{r},\,t)\hat{H}_L(t'')\rangle\\&\quad+\int_{t_0}^{t}\int_{t_0}^{t'}\mathrm{d}t'\mathrm{d}t''\langle\hat{O}(\mathbf{r},\,t)\hat{H}_L(t')\hat{H}_L(t'')\rangle\Bigg)\\&\equiv\int_{t_0}^{\infty}\int_{t_0}^{\infty}\mathrm{d}t'\mathrm{d}t''\chi(t,\,t',\,t'').\end{aligned}\tag{9}$$

A concept similar to the first order susceptibility, namely the second order one, is used here:

$$\begin{aligned}\chi(t,\,t',\,t'')=&\frac{\theta(t-t')\theta(t'-t'')}{(\mathrm{i}\hbar)^2}\\&\times\langle[[\hat{O}(\mathbf{r},\,t),\,\hat{H}_L(t')],\,\hat{H}_L(t'')]\rangle.\end{aligned}\tag{10}$$

2.3. Including the chemical potential and making the rotating wave approximation

Although the initial Hamiltonian (2) is canonical, one would like to include the chemical potentials in order to be able to use, for instance, mean-field descriptions that are done using the grand canonical ensemble. Furthermore, we wish to perform the standard rotating wave approximation to the fields. For these purposes, we consider the fields in the interaction picture as introduced above, $\hat{\psi}_{\sigma C}^{\dagger}(\mathbf{r},\,t) = \mathrm{e}^{\mathrm{i}\hat{H}_{0C}t/\hbar}\hat{\psi}_{\sigma}^{\dagger}(\mathbf{r})\mathrm{e}^{-\mathrm{i}\hat{H}_{0C}t/\hbar}$. In case of electromagnetic fields, the time dependence of the field amplitude $\Omega(\mathbf{r},\,t)$ is harmonic, for instance $\sin(\omega_L t)$. We proceed to do the standard rotating wave approximation: only the resonant terms $\mathrm{e}^{\mathrm{i}(\omega_L-\omega_{eg})t}$ are kept (the non-resonant $\mathrm{e}^{\mathrm{i}(\omega_L+\omega_{eg})t}$ are removed) [15]. We now aim to use operators that are the interaction picture operators but transformed with a grand canonical Hamiltonian. For this purpose a chemical potential term $\sum_\sigma \mu_\sigma\hat{\psi}_{\sigma}^{\dagger}(\mathbf{r})\hat{\psi}_{\sigma}(\mathbf{r})$ is added to the Hamiltonian $\hat{H}_{0C}$: it is also subtracted from it so that nothing has been effectively done. Furthermore, terms proportional to the internal state energy are separated from $\hat{H}_{0C}$. With these manipulations, we have

$$\begin{aligned}\hat{\psi}_{\sigma C}^{\dagger}(\mathbf{r},\,t)&=\mathrm{e}^{\mathrm{i}\hat{H}_{0C}t/\hbar}\hat{\psi}_{\sigma}^{\dagger}(\mathbf{r})\mathrm{e}^{-\mathrm{i}\hat{H}_{0C}t/\hbar}\\&=\mathrm{e}^{\mathrm{i}(E_\sigma+\mu_\sigma)t/\hbar}\mathrm{e}^{\mathrm{i}\hat{H}_0t/\hbar}\hat{\psi}_{\sigma}^{\dagger}(\mathbf{r})\mathrm{e}^{-\mathrm{i}\hat{H}_0t/\hbar}\\&=\mathrm{e}^{\mathrm{i}(E_\sigma+\mu_\sigma)t/\hbar}\hat{\psi}_{g/e}(\mathbf{r},\,t),\end{aligned}\tag{11}$$

where now the operators $\hat{\psi}_{g/e}(\mathbf{r},\,t)$ are the interaction picture operators with respect to a grand canonical Hamiltonian that does not include the field, namely:

$$\begin{aligned}\hat{H}_0=&\int\mathrm{d}\mathbf{r}\sum_\sigma\hat{\psi}_{\sigma}^{\dagger}(\mathbf{r})\left(-\frac{\hbar^2\nabla^2}{2m_\sigma}-\mu_\sigma+V_{T,\sigma}(\mathbf{r})\right)\hat{\psi}_{\sigma}(\mathbf{r})\\&+\frac{1}{2}\sum_{\alpha,\beta}\int\mathrm{d}\mathbf{r}\int\mathrm{d}\mathbf{r}'V_{\alpha\beta}(\mathbf{r},\,\mathbf{r}')\hat{\psi}_{\alpha}^{\dagger}(\mathbf{r})\hat{\psi}_{\beta}^{\dagger}(\mathbf{r}')\hat{\psi}_{\beta}(\mathbf{r}')\hat{\psi}_{\alpha}(\mathbf{r})\end{aligned}\tag{12}$$

This transformation is applied to modify the observable $\langle\hat{N}_e\rangle$ which leads to factors of $\mathrm{e}^{\pm\mathrm{i}(E_e-E_g+\mu_e-\mu_g)t/\hbar}$. Multiplying the $\sin(\omega_L t) = (\mathrm{e}^{\mathrm{i}\omega_L t}-\mathrm{e}^{-\mathrm{i}\omega_L t})/(2\mathrm{i})$ terms with these, one is now able to make the usual rotating wave approximation. In the rotating wave approximation, only terms of the form $\omega_L-(E_e-E_g)/\hbar=\delta$ are considered those with $\omega_L+(E_e-E_g)/\hbar$ are ignored. The chemical potential difference $\mu_g-\mu_e$ now acts in the same way as the detuning δ. This makes it convenient to define a generalized detuning $\tilde{\delta}=\delta+(\mu_g-\mu_e)/\hbar$. The particle number current becomes

$$\begin{aligned}\langle\Psi(t)|\hat{N}_e(t)|\Psi(t)\rangle=&-\frac{1}{4}\int_{t_0}^{t}\mathrm{d}t'\int\mathrm{d}^3r\int\mathrm{d}^3r'\Omega(\mathbf{r})\Omega^*(\mathbf{r}')\\&\times\mathrm{e}^{-\mathrm{i}\tilde{\delta}(t-t')}\langle[\hat{\psi}_e^{\dagger}(\mathbf{r},\,t)\hat{\psi}_g(\mathbf{r},\,t),\,\hat{\psi}_g^{\dagger}(\mathbf{r}',\,t')\hat{\psi}_e(\mathbf{r}',\,t')]\rangle\\&+\mathrm{h.c.}.\end{aligned}\tag{13}$$

The general form of the current, equation (13) describes various types of spectroscopies, only that the species e and g coupled by the fields may be different in each type. Moreover, the $\mathbf{r}$-dependence of the coupling $\Omega(\mathbf{r})$ determines whether momentum is given by the field to the system.

2.4. Linear response with mean-field approximation

In equation (13), correlations arising from operator combinations $\hat{\psi}_\sigma\hat{\psi}_\sigma$ are neglected [1]. Otherwise, however, it is the exact formula for the first order linear response. Further closed formulas for the response can be calculated when one of the states, for instace e, is a non-interacting one (or at least has no interactions with the state g). In other words, only the field couples the states e and g. Then the four-operator correlators can be factorized:

$$\begin{aligned}&\langle[\hat{\psi}_e^{\dagger}(\mathbf{r},\,t)\hat{\psi}_g(\mathbf{r},\,t),\,\hat{\psi}_g^{\dagger}(\mathbf{r}',\,t')\hat{\psi}_e(\mathbf{r}',\,t')]\rangle\\&\quad=\langle\hat{\psi}_e^{\dagger}(\mathbf{r},\,t)\hat{\psi}_e(\mathbf{r}',\,t')\rangle\langle\hat{\psi}_g(\mathbf{r},\,t)\hat{\psi}_g^{\dagger}(\mathbf{r}',\,t')\rangle\\&\qquad-\langle\hat{\psi}_e(\mathbf{r}',\,t')\hat{\psi}_e^{\dagger}(\mathbf{r},\,t)\rangle\langle\hat{\psi}_g^{\dagger}(\mathbf{r}',\,t')\hat{\psi}_g(\mathbf{r},\,t)\rangle.\end{aligned}\tag{14}$$

There are, however, cases when this a factorization is not justifiable, for instance if the final state e interacts strongly with some of the initial states. In that case evaluating the

whole four-operator correlator, for instance using self-consistent schemes, is the way to approach.

2.5. Response for initial BCS state and final normal state

As an illustrative example, let us consider the case when the system is intially in the BCS state. The Bogoliubov transformation [16] gives new quasiparticle operators $\hat{\gamma}$. The relation to the original operators (choosing the species g to be initially in the BCS state, paired with another state g') is $\hat{c}_{lg} = u_l\hat{\gamma}_{lg} + v_l\hat{\gamma}^{\dagger}_{lg'}$. Here u_l and v_l are the Bogoliubov coefficients, and l is a generic index referring to momentum or other quantum number, such as the trap quantum number. It is assumed that the final state in the spectroscopy is non-interacting. Now we apply this simple mean-field theory to the linear response formula, doing the approximation to the factorized form as in equation (14). The current, for species e is in the normal state and g in the BCS one, is now

$$\begin{aligned} I(\tilde{\delta}) = \frac{\pi}{2}\sum_{k,l}\left|\int \mathrm{d}^3r'\Omega(\mathbf{r})\varphi^*_{ke}(\mathbf{r})\varphi_{lg}(\mathbf{r}')\right|^2 \\ \times(-u_l^2 n_{\mathrm{F}}(E_{ke})n_{\mathrm{F}}(E_{lg})\delta((E_{ke}+E_{lg})/\hbar-\tilde{\delta}) \\ - v_l^2 n_{\mathrm{F}}(E_{ke})(1-n_{\mathrm{F}}(E_{lg}))\delta((E_{ke}-E_{lg})/\hbar-\tilde{\delta}) \\ + u_l^2(1-n_{\mathrm{F}}(E_{ke}))(1-n_{\mathrm{F}}(E_{lg})) \\ \times\delta((E_{ke}+E_{lg})/\hbar-\tilde{\delta}) \\ + v_l^2(1-n_{\mathrm{F}}(E_{ke}))n_{\mathrm{F}}(E_{lg})\delta((E_{ke}-E_{lg})/\hbar-\tilde{\delta})). \end{aligned} \tag{15}$$

Here $\varphi_{k\sigma}(\mathbf{r})$ is the basis wave function related to the quantum number k (for instance plane waves or harmonic trap eigenfunctions) and $E_{k\sigma}$ are the quasiparticle energies labelled by k and σ.

The discussion so far has assumed zero temperature. Finite temperatures are often treated with the so-called Matsubara formalism, based on Green's functions. Then the zero-temperature Fermi distributions $n_{\mathrm{F}}(E)$ above are simply the finite temperature distributions. The rest of the results in this article are presented in the finite temperature formalism.

2.6. RF spectroscopy

An RF field can be used to transfer an atom or molecule between two of its internal state (denoted g and e here) to obtain spectroscopic information about the system. The total system may have more species than e and g. Actually, usually one of the species, for instance e, is not present before applying the field. In this case the state e is called the final state (and g would be the initial state). The spatial dependence of the field, $\Omega(\mathbf{r}) = \Omega\exp^{\mathbf{i}\mathbf{k}_L\cdot\mathbf{r}}$ can be simplified in case of RF spectroscopy. The wavelength of the RF field is large compared to size of the atom cloud. This means that the momentum of the RF photon $\mathbf{k}_L$ is negligible compared to the Fermi momentum and one can approximate $k_L \simeq 0$. Also the intensity of the RF field is approximately constant over the cloud. The field amplitude is thus simplified to $\Omega(\mathbf{r}) \simeq \Omega$. A constant field amplitude Ω means that momentum is conserved in the transfer process, as seen equation (15) by calculating the overlap integrals that contain now only the orthonormal basis functions. The momentum of the final particles may or may not be resolved, depending on the case.

The version of RF spectroscopy where momentum is not resolved is, for historical reasons, the 'usual' or 'standard' RF spectroscopy. If both e and g are in a normal state the current is

$$\begin{aligned} I(\tilde{\delta}) = \frac{\pi}{2}\sum_k|\Omega|^2[n_{\mathrm{F}}(E_{kg})(1-n_{\mathrm{F}}(E_{ke})) \\ - n_{\mathrm{F}}(E_{ke})(1-n_{\mathrm{F}}(E_{kg}))] \\ \times\delta((E_{ke}-E_{kg})/\hbar-\tilde{\delta}). \end{aligned} \tag{16}$$

One can make a direct connection to Fermi's golden rule by changing the momentum summation into energy integration, which brings in the density of states. For instance energy shifts caused by interactions can be observed with RF spectroscopy. This is because, if the kinetic and potential energy terms in $(E_{ke}-E_{kg})/\hbar-\tilde{\delta}$ cancel, we obtain $(E_{\mathrm{int},ke}-\mu_e-E_{\mathrm{int},kg}+\mu_g)/\hbar-\tilde{\delta} = (E_{\mathrm{int},ke}-\mu_e-E_{int,kg}+\mu_g)/\hbar-\delta-(\mu_g-\mu_e)/\hbar = (E_{\mathrm{int},ke}-E_{\mathrm{int},kg})/\hbar-\delta$.

An interesting case is the one where one of the states (g) is in a BCS state. Assuming that the final state e is non-interacting and therefore in normal state, one can derive the formula for the current from (15) resulting to

$$\begin{aligned} I(\tilde{\delta}) = \frac{\pi}{2}\sum_k|\Omega|^2(-u_k^2 n_{\mathrm{F}}(E_{ke})n_{\mathrm{F}}(E_{kg})\delta((E_{ke}+E_{kg})/\hbar-\tilde{\delta}) \\ - v_k^2 n_{\mathrm{F}}(E_{ke})(1-n_{\mathrm{F}}(E_{kg}))\delta((E_{ke}-E_{kg})/\hbar-\tilde{\delta}) \\ + u_k^2(1-n_{\mathrm{F}}(E_{ke}))(1-n_{\mathrm{F}}(E_{kg})) \\ \times\delta((E_{ke}+E_{kg})/\hbar-\tilde{\delta}) \\ + v_k^2(1-n_{\mathrm{F}}(E_{ke}))n_{\mathrm{F}}(E_{kg})\delta((E_{ke}-E_{kg})/\hbar-\tilde{\delta})), \end{aligned} \tag{17}$$

using the BCS quasiparticle energy $E_{kg} = \sqrt{\xi_{kg}^2+\Delta^2}$, where Δ is the superfluid order parameter (the excitation gap) and $\xi_{kg} = \epsilon_{kg} - \mu_g$, where ϵ_{kg} is the kinetic energy.

2.6.1. Momentum-resolved RF spectroscopy (photoemission spectroscopy).

In case of momentum resolved spectroscopy, one removes the k-summation from the above formulas. Then one can understand the peak of the resulting spectrum $I(\tilde{\delta}, k) \equiv I(E, k)$ as the dispersion relation $E(k)$. This is the important feature of the momentum-resolved RF spectroscopy: it is quite directly linked to the spectral function $A(k, \omega)$. The spectral function can be defined using Green's functions, it is the imaginary part of the retarded Green's function: $A(k, \omega) = -2\mathcal{I}m(G_{\mathrm{ret}}(k, \omega))$. The final result for momentum-resolved RF spectroscopy is, given in terms of spectral functions as derived in [17] and

[18]:

$$I(\tilde{\delta}, k) = -\frac{1}{4}\sum_{l}\left|\int \mathrm{d}^3 r' \Omega(\mathbf{r})\varphi^*_{ke}(\mathbf{r})\varphi_{lg}(\mathbf{r}')\right|^2 \int_{-\infty}^{\infty}\frac{\mathrm{d}\epsilon}{2\pi}[n_{\mathrm{F}}(\epsilon) - n_{\mathrm{F}}(\epsilon - \tilde{\delta})]A_e(k, \epsilon) \times A_g(l, \epsilon - \tilde{\delta}) = -\frac{|\Omega|^2}{4}[n_{\mathrm{F}}(\xi_k) - n_{\mathrm{F}}(\xi_k - \tilde{\delta})]A_g(k, \xi_k - \tilde{\delta}). \tag{18}$$

The second line follows because for the RF field $\Omega(\mathbf{r}) \simeq \Omega$ (within the scale of the trap) and thus momentum conserved. We have also taken the final state e to be in a normal state for which the spectral function is straightforward: $A_e(k, \epsilon) = 2\pi\delta(\epsilon - \xi_{ke})$. Note that to correspond to the definition of field-matter interaction in equation (1) a factor of $1/4$ is added. As seen from the result (18), the momentum-resolved RF spectrum directly gives the spectral function of the initial state.

2.6.2. Imbalanced gases. The general formalism presented above applies directly to imbalanced gases as well. The only extension needed is to apply the Bogoliubov eigenenergies and eigenfunctions of the imbalanced case. For further information on the details of the Bogoliubov transformation for imbalanced gases, describing a superfluid, see for instance [19]. For the probing of the normal state for imbalanced gases see for instance [20]. For further theory literature on the topic of imbalanced gases see the reviews by Radzihovsky and Sheehy [8], Chevy and Mora [9] and Gubbels and Stoof [10].

2.7. Bragg spectroscopy

Bragg spectroscopy does not change the internal state of the particle and there the field can give a finite amount of momentum q to the particle. Let us associate the initial state with the operator $\hat{c}^\dagger_{kg}$ and the final state with $\hat{c}^\dagger_{k+q,g}$. Typically, the atoms experience two (nearly) counterpropagating laser beams are used so that photons can be absorbed from one beam and emitted to the other. In this process, the atom returns to its initial state in the final emission process. The Bragg process is resonant at the frequency difference $2\hbar k_L^2/m$ between the beams if there are no line shifts due to interactions, etc. Here $2\hbar k_L^2/m$ corresponds to the recoil energy. The detuning δ can be tuned to be larger than this in order to create excitations in an interacting gas.

Density–density correlations and spin susceptibility are the important quantities that can be measured by Bragg spectroscopy. Linear response derivation for Bragg spectroscopy proceeds following the steps outlined in section 2.2. Now that the internal state does not change in the process, one has to modify the description by replacing the label e by g. Note, however, that in a spin-flip process, which is applied when studying spin susceptibility, the label e stays but it now simply means the other component in the gas (say g'). The intermediate state involved in the middle of the Bragg process is adiabatically eliminated, giving an effective coupling of the two-photon transition Ω_{eff} that is proportional to $\Omega_1\Omega_2$, the product of the individual Rabi frequencies. The final effective field coupling becomes $\Omega_{\mathrm{eff}}(\mathbf{r}) = \Omega_{\mathrm{eff}}\cos(\mathbf{q}\cdot\mathbf{r} - \delta t)$.

The response is calculated by evaluating the density (or particle number) as a function of the momentum and energy given, $\mathbf{q}$ and δ, setting $t = 0$ and $t_0 = -\infty$. The essential quantity is now the density–density susceptibility

$$\chi(\mathbf{k}, \omega) = -\frac{1}{\hbar Z}\sum_{m,n}\mathrm{e}^{-\beta E_m}\left[\frac{|\langle m|\hat{n}(\mathbf{k})|n\rangle|^2}{\omega - \omega_{nm} + \mathrm{i}\eta} - \frac{|\langle m|\hat{n}(-\mathbf{k})|n\rangle|^2}{\omega + \omega_{nm} + \mathrm{i}\eta}\right], \tag{19}$$

where Z is the partition function. The Bragg response within linear response theory becomes

$$N(\mathbf{q}, \delta) = \frac{\hbar\Omega_{\mathrm{eff}}}{2}\chi''(\mathbf{q}, \delta), \tag{20}$$

where χ'' is the imaginary part of the density–density susceptibility. It gives the dynamic structure factor $S(\mathbf{q}, \delta)$:

$$\chi''(\mathbf{q}, \delta) = \pi(S(\mathbf{q}, \delta) - S(-\mathbf{q}, -\delta)), \tag{21}$$

which at zero temperature simplifies to

$$\chi''(\mathbf{q}, \delta) = \pi S(\mathbf{q}, \delta). \tag{22}$$

At finite temperature the imaginary part of the susceptibility is

$$\chi''(\mathbf{q}, \delta) = \pi(1 - \mathrm{e}^{-\hbar\delta/(k_B T)})S(\mathbf{q}, \delta). \tag{23}$$

Bragg spectroscopy therefore reveals the dynamic structure factor. The dynamic structure factor incorporates all excitations available in the system at frequency ω and momentum $\mathbf{k}$. In principle, both the density–density correlations and the spin susceptibility are contained in the dynamic structure factor:

$$S(\mathbf{k}, \omega) = S(\mathbf{k}, \omega)_{\uparrow\uparrow} + S(\mathbf{k}, \omega)_{\downarrow\downarrow} + S(\mathbf{k}, \omega)_{\uparrow\downarrow} + S(\mathbf{k}, \omega)_{\downarrow\uparrow}. \tag{24}$$

Experimentally, in case of a specific spectroscopy, one has to pay attention to the coupling of the perturbation. It may couple to the density or the spin or both. Importantly, the Bragg response contains both single particle and collective excitations of the systems. For further information, see [1], section 10.5.4. A derivation of the Bragg spectroscopy response by perturbation theory, using a slightly different approach from the one in [1], can be found in the book by Pitaevskii and Stringari [21].

2.8. Lattice modulation spectroscopy

In the lattice modulation spectroscopy, the light potential that traps the particles into a lattice configuration is modulated with the frequency ω_L. The potential is coupled to the density and thereby excites the system.

Let us now consider a Hubbard type Hamiltonian in the lattice basis. The tunnelling within the tight-binding approximation is described by the energy J, and U is the onsite interaction energy. Modulation of the trap potential follows

the function $g(t)$. The Hamiltonian is

$$\hat{H} = -J\hat{H}_K + U\hat{H}_U + g(t)\hat{H}_K, \tag{25}$$

$$\hat{H}_K = \sum_{\langle i,j,\rangle\sigma} \hat{c}^{\dagger}_{j\sigma}\hat{c}_{i\sigma} + \text{h.c.}, \tag{26}$$

$$\hat{H}_U = \sum_{i,\sigma,\sigma'} u_{\sigma\sigma'}\hat{n}_{i\sigma}\hat{n}_{i\sigma'}, \tag{27}$$

where $u_{\sigma\sigma'}$ tells which types of interactions are present. For bosons, the relevant observable can be the heating caused by the lattice modulation. This is not, however, straightforward to detect in case of fermions, so another observable is needed. The double occupancy $\hat{D} = \sum_i \hat{n}_{i\sigma}\hat{n}_{i\sigma'}$ is able to provide useful information about the response. As this observable does not include the field, the first order perturbation terms in equation (8) are not sufficient. Applying the second order ones, the double occupancy becomes (choose $t_0 = -\infty$)

$$\langle\Psi(t)|\hat{D}(t)|\Psi(t)\rangle = \int_{-\infty}^{\infty}\int_{-\infty}^{\infty} \mathrm{d}t'\mathrm{d}t'' g(t')g(t'')\chi(t, t', t''). \tag{28}$$

Here we now have the second order susceptibility instead of the first order one:

$$\chi(t, t', t'') = -\frac{\theta(t-t')\theta(t'-t'')}{\hbar^2} \times \langle[[\hat{H}_U(t), \hat{H}_K(t')], \hat{H}_K(t'')]\rangle. \tag{29}$$

Some terms from this expression average to zero so that only the non-oscillating term remains [22]

$$\langle\Psi(t)|\hat{D}(t)|\Psi(t)\rangle = \langle\Psi(0)|\hat{D}(0)|\Psi(0)\rangle - \frac{1}{2U}g(0)^2\omega t\mathcal{I}m\chi_K(\omega). \tag{30}$$

Here $\chi_K(\omega)$ is obtained from $\chi(t) = (1/\hbar)\langle[H_K(t), H_K(0)]\rangle$ by a Fourier transform.

3. Early theory for spectroscopies of ultracold Fermi gases

3.1. Spectroscopy for measuring the pairing gap

In the year 2000, Törmä and Zoller suggested that the pairing gap in attractively interacting Fermi gases could be probed spectroscopically [17]. This work provides the basic theory results for RF spectroscopy response for superfluids within the BCS theory. Originally, Raman spectroscopy was suggested in [17] but the concept and the theory description is are the same independent of whether RF field or a Raman configuration is used.

For trapped ultracold gases, the trapping geometry, often harmonic, may affect the spectroscopy. Reference [17] gave results both for a homogeneous system and for the trapped case where the basis states are the harmonic oscillator states instead of the plane waves. The trapped case was considered in more depth by Bruun, Törmä, Rodríguez and Zoller [18], and also in later works by Ohashi and Griffin [23] and He, Chen and Levin [24]. Another approach is the local density approximation. The external potential is assumed to be locally constant and is taken into account only as a simple shift in the chemical potential, $\mu_{\text{eff}} = \mu - V_T(\mathbf{x})$. Now one can calculate the spectra for each position simply using $\mu_{\text{eff}}(\mathbf{x})$ and the homogeneous case formulas. The results can finally be averaged over all positions in the trap. Local density approximation was used by Kinnunen, Rodrígues and Törmä in [25] and in many subsequent works.

The equations (15), (17) and (18) are given by [17]. They predict that in an experiment, in case of BCS pairing, the spectral peak that would in non-interacting case coincide with zero detuning $\delta = 0$ will shift. Also the shape of the peak changes since the density of states has a gap and corresponding strong peaks at the edges of the gapped area. Intuitively, one can think that the probing field has to provide extra energy to break a Cooper pair so that is it possible to transfer a particle to a third state that is not part of the superfluid state. Thus there is a threshold for the RF response.

3.2. RF threshold

Choosing $\delta > 0$ and assuming a constant density of states ρ, as well as no particles initially in the non-interacting e final state, at zero temperature one obtains [17] from (17)

$$I(\delta) = \frac{\pi\Omega^2}{2\hbar}\rho\theta(\delta^2 - \Delta^2/\hbar^2 + 2\delta\mu/\hbar)\frac{\Delta^2}{\delta^2}, \tag{31}$$

where θ is the Heaviside step function. Applying the actual density of states of the BCS state brings in the particle mass m and the system volume V. The result becomes [17, 18]

$$I(\delta) = \frac{\Omega^2 V m^{3/2}}{4\pi\hbar^{7/2}}\theta(\delta^2 - \Delta^2/\hbar^2 + 2\delta\mu/\hbar) \times \frac{\Delta^2}{\delta^2}\sqrt{\frac{\delta^2 - \Delta^2/\hbar^2}{\delta} + 2\frac{\mu}{\hbar}}. \tag{32}$$

Here one could also use $k_{\text{F}}^3 = 3\pi^2 N/V$ where N is the total particle number. Let us now discuss three important issues that can be observed from these results.

Firstly, the equations (31) and (32) give the threshold for the RF response. It is set by the theta-function and becomes [17]

$$\hbar\delta_{\text{threshold}} = \sqrt{\mu^2 + \Delta^2} - \mu. \tag{33}$$

The threshold does not equal the gap energy. This is because the final state is initially empty and the smallest energies for particle transfer are given by the particles in the lowest momentum states. The chemical potential can include the Hartree energy, which thereby also affects the threshold. Note that approximately (Taylor expansion) $\hbar\delta_{\text{threshold}} \sim \Delta^2/(2\mu)$ $\sim \Delta^2/(2E_{\text{F}})$ although one should be cautious with this since in unitary Fermi gases the gap is not extremely small compared to the chemical potential, and the chemical potential and the Fermi energy deviate from each other considerably. In case the final state is occupied to the same Fermi level as the rest of the gas, only particles near the Fermi level are transferred. Then $\hbar\delta = \Delta$ is the threshold. In this way the gap energy could be directly obtained, in a way similar to the gap

measured in the superconductor-normal metal tunnelling experiments by Giaver [26].

The second observation is that the equation (32) gives the high-energy tail of the spectrum. Assuming large δ drops out all but the $\sqrt{\delta}$ contribution in the square root term of equation (32). The approximate form of the equation becomes

$$I(\delta)_{\delta\to\infty} = \frac{\Omega^2 V\sqrt{\hbar}}{4\pi\sqrt{m}}\frac{m^2\Delta^2}{\hbar^4}\frac{1}{\delta^{3/2}}. \tag{34}$$

The power-law dependence of the tail of the RF spectrum $I(\omega)$ is thus $\omega^{-3/2}$. Note that this result is derived within the BCS theory which treats normal-state interparticle interactions with a simple Hartree approach where they merely shift the chemical potential. More accurate derivation of the tail of the RF spectrum can be done using the concept of contact, see section 12, equation (42), which shows that the tail is proportional to the contact. The contact contains both pairing contributions, related to Δ, and Hartree-type interaction effects also present in the normal state. Far in the BCS limit where the scattering length $a \to 0$ and Δ is exponentially suppressed, the result derived using the contact shows that the tail becomes proportional to an^2 where n is the density.

Finally, the equations (31) (and (32)) shows that, within the simple BCS theory, the current is directly proportional to the square of the pairing gap Δ^2.

Note that the decay of the tail is in contrast to the superconductor—normal metal experiments where the current simply grows after the threshold. This is explained by the difference that momentum is not conserved in the tunnelling (particle transfer) process, while RF spectroscopy preserves momentum.

3.3. Early theory work on Bragg spectroscopy

In the context of ultracold Fermi gases, some of the first studies considering the prospects of Bragg spectroscopy theoretically are by Minguzzi, Ferrari and Castin [27], Rodríguez and Törmä [28], Büchler, Zoller and Zwerger [29], Bruun and Baym [30], Combescot, Giorgini and Stringari [31], and Challis, Ballagh and Gardiner [32].

4. Early RF spectroscopy experiments: mean-field effects

RF spectroscopy has been used for probing condensates of bosonic atoms since the early days of alkali BECs (see, e.g., the introduction in [33]) Concerning studies of fermionic many-body physics, the pioneering experiments on the use of RF spectroscopy were the works of Regal and Jin [34] and Gupta, Ketterle and coworkers [33] in the year 2003. In these works, RF spectroscopy was used to study mean-field energies in strongly interacting Fermi gases. In [34] ^{40}K atoms in two hyperfine states $|F = 9/2, m_F = -9/2\rangle$ and $|9/2, -7/2\rangle$ were prepared. The atoms were basically non-interacting. Then an RF pulse was applied to move atoms from the state the $|9/2, -7/2\rangle$ to the state $|9/2, -5/2\rangle$ which was strongly interacting with atoms in state $|9/2, -9/2\rangle$ due to a Feshbach resonance. The resulting mean-field energy shift, see equation (16) and the discussion following it, was observed. In [33], the system was prepared in a mixture of two lowest hyperfine states of ^{6}Li, $|1/2, 1/2\rangle \equiv |1\rangle$ and $|1/2, -1/2\rangle \equiv |2\rangle$ and an RF pulse was applied between the latter and a third state, $|3/2, -3/2\rangle \equiv |3\rangle$, to observe mean-field shifts in the energy (the shorthand notation $|1\rangle, |2\rangle, |3\rangle$ for ^{6}Li will be used later in this article). Also another experiment, tranferring atoms initially in the state ^{6}Li, $|1/2, 1/2\rangle$ to the state $|1/2, -1/2\rangle$ with an RF pulse, was performed and resulted in a totally different outcome, as discussed in the following section.

4.1. RF spectroscopy reveals symmetries of the Hamiltonian

In ultracold gas spectroscopies, the process can often be highly coherent. When applying a field that couples atoms in an internal state g to another one, say e, for a certain time duration τ, for each atom a coherent superposition $a(\tau)|g\rangle + b(\tau)|e\rangle$ of the two internal states is created. This corresponds to a rotation in the space spanned by the two states. Now if the Hamiltonian of the system has symmetries that are related to the applied rotation, one has to be cautious. It is important to check whether the Hamiltonian is invariant under the rotation. An intriguing experimental example of this is presented by Gupta, Hadzibabic, Zwierlein and Ketterle, first in [33], and then in [35] which also contains a theoretical analysis of the phenomenon. In [35] a two-component (here labeled g and e) Fermi gas is considered. The many-body Hamiltonian (see equation (1); contact interaction and no trap potential are assumed) of the system, with no field, is

$$\hat{H}_C = \int \mathrm{d}^3 r \sum_{\sigma=e,g} \hat{\psi}_\sigma^\dagger(\mathbf{r})\left(-\frac{\hbar^2\nabla^2}{2m_\sigma} + E_\sigma\right)\hat{\psi}_\sigma(\mathbf{r}) + V\int \mathrm{d}^3 r \hat{\psi}_e^\dagger(\mathbf{r})\hat{\psi}_g^\dagger(\mathbf{r})\hat{\psi}_g(\mathbf{r})\hat{\psi}_e(\mathbf{r}). \tag{35}$$

Assuming Hartree energy given by mean-field theory (but no pairing), the interaction term of the last line of equation (35) means that the component g has a simple form of interaction energy: $E_{\mathrm{int}} = Vn_e\hat{\psi}_g^\dagger\hat{\psi}_g$ where $n_e = \langle\hat{\psi}_e^\dagger\hat{\psi}_e\rangle$. If all atoms are initially in state g, then $n_e = 0$ means that $E_{\mathrm{int}} = 0$. Now think that one particle would be transferred to the state e: clearly E_{int} is finite. Correspondingly, the frequency required to transfer the particle from one internal state to another should be shifted from $\delta = 0$ to $\delta - E_{\mathrm{int}} = 0$. However, the case where the gas is probed by a coherent field actually produces a completely different result. The coherent rotation caused by the field can be parametrized by angles θ and ϕ:

$$\hat{\psi}_1 = \cos(\theta/2)\mathrm{e}^{\phi/2}\hat{\psi}_g + \sin(\theta/2)\mathrm{e}^{-\phi/2}\hat{\psi}_e, \tag{36}$$

$$\hat{\psi}_2 = -\sin(\theta/2)\mathrm{e}^{\phi/2}\hat{\psi}_g + \cos(\theta/2)\mathrm{e}^{-\phi/2}\hat{\psi}_e. \tag{37}$$

Applying this transformation to the Hamiltonian (35) actually keeps the Hamiltonian unchanged. This was indeed observed in the experiments: the RF transfer between the states $|1\rangle$ and $|2\rangle$ did not show any interaction energy shift in [33]. In the further study [35], the same group connected the absence of the mean-field energy shift to the symmetries of the

Hamiltonian and thereby showed that no shifts should be observed even in the case of a paired superfluid. Analogous phenomena have been observed in NMR experiments of ^{3}He superfluids by Osheroff, Gully, Richardson, and Lee [36]. There, in an NMR experiment a coherent superposition of two spin states is created in a similar way as in the RF spectroscopy experiments here. If the Hamiltonian is symmetric with respect to the rotation, no shifts are expected. The appearance of a shift in [36] for certain parameter regimes was suggested by Leggett [37] to be related to spontaneous breaking of the symmetry in question, such as an unisotropic BCS-type superfluid with pairing in a higher angular momentum state. Note that in a typical ultracold gas Fermi superfluid, any shifts should be absent, as mentioned above. This is because even when the superfluid has a spontaneously broken symmetry in the global phase, it is still symmetric with respect to a coherent rotation of the components, see above. In a usual *s*-wave BCS superfluid, one can rotate the spins to a new basis, and the physics will be the same. This is, however, not necessarily the case for more complicated superfluids, such as the ^{3}He example.

5. RF spectroscopy in understanding the BCS–BEC crossover: experiments and theory using the density balanced gas

5.1. The pioneering experiments

Fermionic many-body pairing and superfluidity in ultracold gases was gradually established during 2003–2005 by contributions from several groups. Insprired by predictions of superfluidity in ultracold Fermi gases by Houbiers, Stoof, Hulet and coworkers [38], and by the breakthrough experiment reaching Fermi degeneracy of potassium atoms by DeMarco and Jin [39], the field had set going in the late 1990s. One great achievement of the ultracold Fermi gas research so far is the experimental verification of the BCS–BEC crossover. Already in the 1960s and 1980s it was suggested by Keldysh (see [40]), Eagles [41], Leggett [42], and Nozieres and Schmitt-Rink [43] that the apparently different phenomena of superconductivity as condensation of delocalized Cooper pairs and BEC of tightly bound, localized pairs (such as molecules) could actually be connected to each other via a smooth crossover. Leggett showed that the simple wavefunctions describing both ends, $|\Psi\rangle_{\rm BEC}$ and $|\Psi\rangle_{\rm BCS}$, are actually smoothly connected to each other, that is

$$|\Psi\rangle_{\rm BEC} = \mathcal{N}\mathrm{e}^{\lambda\sum_{\mathbf{k}}\varphi_{\mathbf{k}}\hat{c}^{\dagger}_{\mathbf{k}\uparrow}\hat{c}^{\dagger}_{-\mathbf{k}\downarrow}}|0\rangle = \prod_{\mathbf{k}}\,(u_{\mathbf{k}} + v_{\mathbf{k}}\hat{c}^{\dagger}_{\mathbf{k}\uparrow}\hat{c}^{\dagger}_{-\mathbf{k}\downarrow})|0\rangle = |\Psi\rangle_{\rm BCS}, \qquad (38)$$

if one requires $v_{\mathbf{k}}/u_{\mathbf{k}} = \lambda\varphi_{\mathbf{k}}$ and $\mathcal{N} = \prod_{\mathbf{k}} u_{\mathbf{k}}$. Here $\varphi_{\mathbf{k}}$ describe the internal structure of the composite boson, $|\lambda|$ divided by the volume gives the condensate fraction, and $v_{\mathbf{k}}$, $u_{\mathbf{k}}$ are the BCS coherence factors (for more details see, e.g., [5] or [44]).

However, these arguments were based on mean-field theory, with approximate ways of including fluctuations; exact calculations of the intermediate regime between the BCS and BEC regimes, at finite temperature, are exceedingly difficult. Experimentally it was difficult to find a system where one could tune the parameters in a controlled and continuous manner: the various types of superconductors and superfluids discovered were naturally in a certain place in the crossover and dramatic tuning of the interaction was not possible [45]. Therefore it remained as an open question whether the transition from one regime to the other is a smooth crossover or whether, for instance, quantum phase transitions occur. It was only when the ultracold Fermi gas experiments arrived that the existence of the crossover could be confirmed experimentally.

Basically, the achievement of fermionic pairing and superfluidity went hand in hand with the studies of the BCS–BEC crossover in ultracold Fermi gases. Molecule formation at the BEC side of the crossover was first observed by the groups of Jin, Hulet, Salomon and Grimm, see Regal *et al* [46], Strecker *et al* [47], Cubizolles *et al* [48] and Jochim *et al* [49]. Such molecules were found to form a BEC by Jochim, Grimm and coworkers [50], Regal, Greiner and Jin [51] and Zwierlein, Ketterle and coworkers [52]. Condensation of pairs at the unitarity regime between the BCS and BEC sides was achieved by Regal, Greiner and Jin [53] and Zwierlein, Ketterle and coworkers [54]. The whole crossover was studied in various experiments showing, among other things, continuous development of the critical temperature, collective modes, and pairing energies over the crossover, by Bartenstein, Grimm and coworkers [55], Kinast, Thomas and coworkers [56] and Bourdel, Salomon and coworkers [57]. The smoking gun proof of superfluidity of the gas was provided by the experiment by Zwierlein, Ketterle and coworkers [58, 59] where quantized vorticies were observed throughout the crossover.

Here, I will say a few more words about a work which was one of the crucial experiments establishing the crossover and where RF spectroscopy was used. In 2004, RF spectroscopy revealed signatures of fermionic many-body pairing in a strongly interacting Fermi gas in an experiment by Chin, Grimm and coworkers [60]. As discussed above (equations (17), (31)–(33)), existence of a pairing gap should lead to a shift of the RF response with respect to the non-interacting case. Indeed a shift in the response was observed when the gas was cooled down, see figure 2. It was also observed that the shift was proportional to the Fermi energy: this showed that non-trivial fermion pairing was taking place instead of only molecule formation, where the binding energy also leads to shifts in RF spectra [61, 62] but with no significant dependence on density. Interestingly, the spectra at higher temperatures displayed a two-peak structure as visible in figure 2. In an accompanying work, Kinnunen, Rodrígues and Törmä [25] provided a theoretical framework which supported the conclusion that the two peaks originate from paired particles in the middle of the harmonic trap and unpaired ones at the edges. The density of particles decreases in a harmonic trap from the centre towards the edges, and with it also the critical temperature related to many-body pairing. In the lowest

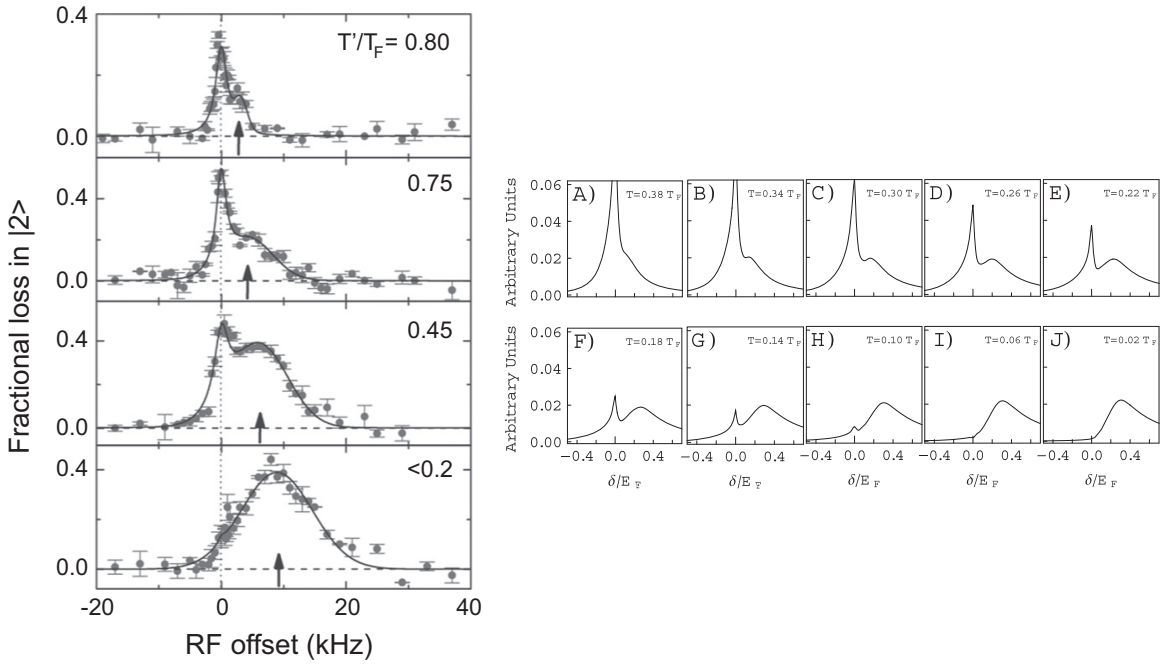

Figure 2. Left: RF spectroscopy was used in [60] to study many-body pairing of fermions. The shift of the peak away from zero RF offset (detuning) reflects pairing which emerges when temperature is lowered. Reproduced with permission from Chin *et al* [60]. Copyright AAAS 2004. Right: theoretical modelling of the spectra in [25]. The double peak structure originates from paired particles in the middle of the trap and unpaired ones (the zero detuning $\delta = 0$ peak) at the trap edges where the local chemical potential is lower. Here T_F is the Fermi temperature. Reproduced with permission from Kinnunen *et al* [25]. Copyright AAAS 2004.

temperatures, only one peak was observed. Other theory work following the experiment by He, Chen and Levin [24], and Ohashi and Griffin [23, 63] reached similar conclusions.

The standard RF spectroscopy basically gives the spectral function $A(\mathbf{k}, \omega)$ integrated over the momentum $\mathbf{k}$. Therefore the experiment [60] was somewhat analogous to the first tunnelling spectroscopy measurements by Giaver that revealed the pairing gap in superconductors [26]. However, the RF response has a spectral shape different from the IV-curve due to momentum conservation in the spectroscopy [17]; the IV curve has an onset at the gap energy and thereafter simply grows, while as seen in figure 2, the RF response has a decaying tail. This tail, exactly due to the momentum conservation, actually contains interesting information, as will be discussed in section 12 of this article.

Although trapping effects may be considered even helpful in analysing the RF spectroscopy experiments, such as the case of the two peaks discussed above, it is desirable to be able to probe also the bulk properties of the gas without trap averaging. Shin, Ketterle and coworkers developed in 2007 a tomographic version of RF spectroscopy [64] which is very powerful since it is spatially resolved: different spatial locations of the trap correspond to different densities, thereby one receives information, for instance about pairing, that corresponds to bulk systems with different chemical potentials. This thinking, of course, assumes that the local density approximation is valid. In 2012, Sagi, Jin and coworkers developed another method to avoid trap averaging in RF spectroscopy [65]: they intersect two perpendicularly propagating hollow light beams that optically pump atoms at the edge of the cloud into a spin state that is dark to the detection.

5.2. Exploring fermion pairing by RF spectroscopy

In section 2.4, it was discussed that the simple factorization of the four-point correlator in equation (14) is accurate only if the final state in the spectroscopy does not significantly interact with the rest of the system. Sometimes this is, however, not the case in ultracold gases. For instance in case of ^{6}Li, if one uses in RF spectroscopy the hyperfine states $|1\rangle$ ($|F = 1/2, m_F = 1/2\rangle$) and $|2\rangle$ ($|F = 1/2, m_F = -1/2\rangle$) as the ones that are strongly interacting or paired, and as the final state the state $|3\rangle$ ($|F = 3/2, m_F = -3/2\rangle$) (as is the case in [33] and [60] and several subsequent works), then final state interactions cannot be neglected.

It was pointed out by Yu and Baym that final state interactions should be taken into account in extracting the value of the pairing gap from RF data [66]. This can be done with the help of elaborate theoretical analysis as in the theory work of Perali, Pieri and Strinati [67, 68], and the work combining experiment and theory by the Grimm and Strinati groups [69]. The other option is to avoid final-state

interactions altogether. For ^{40}K, final state interactions can be neglected because the Feshbach resonances are narrow and there are no overlaps between different resonances. Concerning ^{6}Li, Schunck, Ketterle and coworkers discovered that if one uses $|1\rangle$ and $|3\rangle$ as the initial states and $|2\rangle$ as the final one, the final state interactions become negligible [70]. This is because ^{6}Li has broad resonances and the ones between $|1\rangle$ and $|2\rangle$ as well as $|2\rangle$ and $|3\rangle$ are partly overlapping while the $|1\rangle$ and $|3\rangle$ resonance is well separated in magnetic field from the others. They used RF spectroscopy in this new setting to determine the fermion pair size. Knowing μ, one can obtain the gap Δ from observing the threshold, equation (33). Such a threshold and RF line shapes of the form of equations (31) and (32) were observed in [71], as will be discussed in section 7.

Sum rules can be used for finding the average peak position in RF spectroscopy. This was done by Yu and Baym [66] (see also the works of Punk and Zwerger [72], Baym, Pethick, Yu and Zwierlein [73], and Basu and Mueller [74]). When there are strong final state interactions, the spectrum is expected to be quite symmetric, and the result becomes (in the notation of [66])

$$\delta_{\text{peak}} = (g_{eg} - g_{gg'})\frac{\Delta^2}{n_0 g_{eg} g_{gg'}}, \tag{39}$$

where g_{eg} is the interaction coupling between the initial and final states and $g_{gg'}$ marks the coupling responsible for the BCS pairing between the initial state and the other component of the gas (g'), and n_0 is the density. From equation (39) one can see that if the symmetry of the Hamiltonian is preserved under the perturbation, here the case is $g_{eg} = g_{gg'}$, there is no shift; this is consistent with the discussion in section 4.1. Furthermore, the peak position is proportional to Δ^2. If there are no final state interactions ($g_{eg} = 0$), the derivation in sections 2.6 and 3.2, following to the early work by Törmä and coworkers [17, 18], gives the threshold of equation (33), namely $\hbar\delta_{\text{threshold}} = \sqrt{\mu^2 + \Delta^2} - \mu \simeq \frac{\Delta^2}{2\mu}$. Therefore, both in cases of finite and no final state interactions there is a Δ^2 dependence, although there is no direct comparison since (39) is not valid for $g_{eg} = 0$. Similarly as discussed after equation (34), this is a BCS derivation, and the more accurate result contains the contact, see equation (43) in section 12.

In case of no final-state interactions, $g_{eg} = 0$, the spectrum has an asymmetric shape with a long, slowly decaying tail. Sum-rule given mean values of the response then become cut-off-dependent within the BCS theory [66]. Thus for such shapes a mean value of the frequency is not a useful characterization and other approaches are preferred over sum rules, such as those discussed in sections 2.6 and 3.2.

5.3. Momentum-resolved RF spectroscopy (photoemission spectroscopy)

A momentum-resolved version of RF spectroscopy was introduced by Stewart, Gaebler and Jin [75]. Avoiding the momentum integration, the spectral function $A(\mathbf{k}, \omega)$ was directly observed in the experiment. In this sense, momentum-resolved RF spectroscopy is analogous to angle-resolved photo-emission spectroscopy; for further information see for instance [6, 11]

5.4. Beyond BCS theory

All the analytical results in sections 2.6 and 3.2 in this article are based on the BCS mean-field theory. Although this is instrutive to understand what kind of qualitative behaviour might be expected from spectroscopies, strongly interacting ultracold Fermi gases are obviously asking for beyond mean-field theoretical treatments. Simple mean-field theories are based on having well-defined quasiparticles and this assumption might not be valid in strongly interacting systems. Even if yes, the properties of the quasiparticles may have to be evaluated beyond BCS theory. The BCS–BEC crossover at low temperature is surprisingly well qualitatively described by the BCS–Leggett theory. But at higher temperatures the quantitative agreement is not good.

Theoretical calculations of RF spectra, with the correlators evaluated with various many-body theories and approaches that go beyond the simple BCS theory are presented for instance in [24, 25, 67, 76–78] and in other works by these and several other groups. In particular, it was noted by Kinnunen, Rodrígues and Törmä [25, 76] and by He, Chen and Levin [24] that since pairing features may appear also above T_c in beyond-BCS scenarios, the shift of the RF spectral peak may appear already in the normal state and is thus not alone a signature of superfluidity.

6. Spin-imbalanced Fermi gases

Although the topics discussed from here on are conceptually very related to the ones above, I separate them to a dedicated section because imposing a spin-density imbalance in a Fermi gas has spun off such an enourmous amount of interesting physics and perspectives, many still unexplored. In ultracold gases, it is possible to prepare an initial condition with different amounts of particles in different internal states (species). In ultracold Fermi gases, such studies were pioneered by experiments published in 2006 by Zwierlein, Shin, Ketterle and coworkers [59, 79], and by Partridge, Hulet and coworkers [80]. In [59], the stability of vortices was studied as a function of polarization $P = (n_\uparrow - n_\downarrow)/(n_\uparrow + n_\downarrow)$ where n_σ are the densities of the species, that is, the spin-density imbalance, on both sides of the BCS–BEC crossover. The famous Chandrasekhar–Clogston limit [81, 82] of chemical potential imbalance that destroys fermionic superfluidity was observed, leading to a critical polarization of about 0.8 in a harmonic trap in the works [59, 79]. Similar critical polarization was later obtained in the experiments by Nascimbène, Salomon and coworkers [83], and was also confirmed with quantum Monte Carlo calculations by Lobo, Recati, Giorgini and Stringari [84], and by a dynamical mean-field theory method by Kim, Kinnunen, Martikainen and Törmä [85]. In [80], a critical polarization close to one was reported, but it

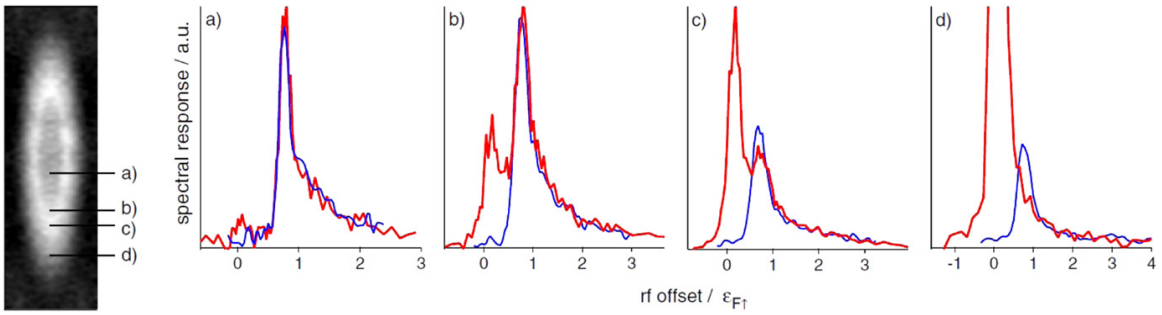

Figure 3. (a) RF spectra from [71] for increasing local polarizations ranging from near zero in (a) and 0.64 in (d). The red curve is the majority spectrum and the blue the minority. Different polarizations are naturally obtained by considering spectra from different areas in the trapped gas, see the leftmost picture. In panels (b) and (c), the majority component shows both pairing and quasiparticles; from such data, values of the pairing gap and Hartree energy can be extracted. In (d), the majority component does not show a peak feature under the minority peak which indicates that polaron-type physics takes place instead of pairing. Reproduced with permission from Schirotzek *et al* [71]. Copyright APS 2008.

was later found to be due to depolarization in the evaporative cooling process [86, 87].

The work by Shin, Ketterle and coworkers in 2008 [88] established by tomographic imaging of the densities that, in a harmonic trap, there is a balanced superfluid in the middle, then a sharp change, reflecting a first order phase transition, to a partially polarized normal state. Finally, at the very edges of the trap, the gas is fully polarized. The normal gas in the edges allows very accurate determination of temperature from cloud profiles. Utilizing this, Shin *et al* determined the critical temperature of a balanced unitary Fermi gas to be $T_c/T_F \simeq 0.15$, where $T_F = (\hbar^2/2mk_B)(6\pi^2 n_\sigma)^{2/3}$ is the Fermi temperature of the gas, m the mass, and n_σ the density of one species. This is very close to values given by various theoretical approaches and later experiments.

The spin-imbalanced gases offered new interesting prospects for the use of spectroscopies as well, in particular precision measurements of the quasiparticle energies and the pairing gap and the studies of polarons, which will be discussed below.

7. Quasiparticle spectroscopy utilizing the spin-imbalance

An important work where spectrocopies were heavily utilized is the one by Schirotzek, Ketterle and coworkers [71]. There tomographic RF spectroscopy was used in different areas of the trap: the fully balanced middle part and various polarized areas around it. Majority and minority spectra were separately analysed: in the balanced case, both spectra overlap and show a shift due to pairing, while in the imbalanced case unpaired majority particles show a contribution with no shift. Intriguinly, the chemical potential imbalance induces quasiparticles in the middle superfluid region already at a low temperature [89]. Therefore Schirotzerk *et al* were able to measure accurately the quasiparticle energies by the RF spectroscopy, see figure 3. According to the predictions by Törmä, Zoller, Bruun and Rodríguez [17, 18], the quasiparticle energies $E_k = \sqrt{\Delta^2 + (\epsilon_k + U - \mu)^2}$, where U is the Hartree energy, appear in the RF spectra according to equations (17), (31)–(33). This allows extracting the pairing gap and the Hartree shift in high precision from the RF spectra. Schirotzek *et al* obtained $\Delta = 0.44(3)\,\epsilon_{F\uparrow}$ and $U = -0.43(3)\,\epsilon_{F\uparrow}$ which are in excellent agreement with the value $\Delta \simeq 0.46\epsilon_{F\uparrow}$ predicted by a Luttinger–Ward approach by Haussmann, Zwerger and coworkers [90] and by quantum Monte Carlo calculations by Carlson and Reddy [91]. By studying the extremely polarized gas, the work [71] contributed to the start of polaron physics studies in ultracold Fermi gases.

8. Spectroscopies in polaron studies

The research on imbalanced Fermi gases naturally led to polaron studies. Thinking in terms of a single impurity immersed in a system, in order to reveal information about the ground state or even excitations, has been a very powerful approach in physics. Sometimes the behaviour of the impurity can be effectively described by the concept of a polaron: an object that deforms its surroundings slightly, causing for instance excitations, and thereby obtains an effective mass different from the bare mass of the impurity. A polaron fulfils the Fermi liquid paradigm and is associated with a quasiparticle weight/residue.

It turned out that at the limit of large polarization (large imbalance), the physics of the ultracold Fermi gas is well described by polaron physics. Throughout the BCS–BEC crossover, there is a non-trivial evolution to a bound molecule. We do not discuss here all the important theory and experiments on this topic but refer to excellent reviews by Chevy and Mora [9] and by Massignan, Zaccanti and Bruun [12]. We only wish to point out those experiments where spectroscopies provided crucial insight to polaron physics.

Schirotzek, Zwierlein and coworkers measured the polaron energies in [92] by using RF spectroscopy. The RF

spectra of the minority species revealed not only the polaron energy, but also the quasiparticle weight or quasiparticle residue Z: it is basically given by the spectral weight under the narrow quasiparticle peak in comparison to a broad incoherent background. They also observed that, during the BCS–BEC crossover, the Fermi polaron transfers into a bound molecule and this is connected to a quantum phase transition from a Fermi gas to a coexistence of Bose and Fermi gases.

In May 2012, two breakthrough works using RF spectroscopy to study polarons were published back-to-back in Nature, namely a study of ^{6}Li–^{40}K mixture by Kohstall, Grimm and coworkers [93], and experiments on a 2D ultracold ^{40}K gas by Koschorrek, Köhl and coworkers [94].

Kohstall *et al* studied polaron energies with RF spectroscopy in a system where the majority atoms were ^{6}Li but the minority was another, heavier, species namely ^{40}K. RF spectroscopy is typically done, as discussed already many times in this article, in such a way that particles in a species that is strongly interacting with another species are transferred by the RF pulse to a third state. Kohstall *et al* did it, however, the other way round: they started with an initial state of potassium that does not interact strongly with lithium, and then transferred the potassium atoms (which were only a small amount, corresponding to the polaron/impurity limit) to a state that has a Feshbach resonance and thus interacts strongly with the lithium internal state. For historical reasons, this is called the *inverse RF spectroscopy* (curiously, the very first RF spectroscopy experiment on Fermi gases by Regal and Jin [34] also used the 'inverse' version, but since then all the works used the 'standard' RF spectroscopy until the work of Kohstall *et al*). One remarkable aspect of the inverse RF spectroscopy is that it can easily probe excitations of the system: while in the usual version one typically probes properties of the ground state, and of the excitations present due to the (low) temperature, with the inverse process it is easy to provide the right amount of energy by the RF field to create a specific excitation of the interacting system. Kohstall *et al* studied the whole crossover from attractive to repulsive polarons, and observed the polaron branches as well as a molecule-hole continuum.

The work by Koschorrek *et al* [94] also explored both the repulsive and attractive polarons. They used momentum-resolved RF spectroscopy (momentum-resolved photo-emission spectroscopy), which directly gives the single particle spectral functions, to study how the polaron energy behaves in two dimensions. Note that in two dimensions, a bound state (molecule) exists throughout the crossover and competes with the polaron branches. The repulsive polaron branch decay times were determined.

9. Two-dimensional gases: studies of polarons and interaction energies by spectroscopies

RF spectroscopy was used for measuring interaction energies and confinement induced resonances in a two-dimensional Fermi gas by Fröhlich, Köhl and coworkers [95]. Sommer, Zwierlein and coworkers studied the interaction and binding energies over the 2D–3D crossover [96]. RF spectroscopy was also used for studying quasi-2D Fermi gases by Zhang, Thomas and coworkers [97]. They discovered polaron states also in the quasi-2D setting. More about all these, and other work on 2D gases which did not use spectroscopies, can be read from the review by Levinsen and Parish [13] and from, for instance, the recent work by Murthy, Jochim and coworkers [98] observing the Berezinskii–Kosterlitz–Thouless transition in a two-dimensinal Fermi gas.

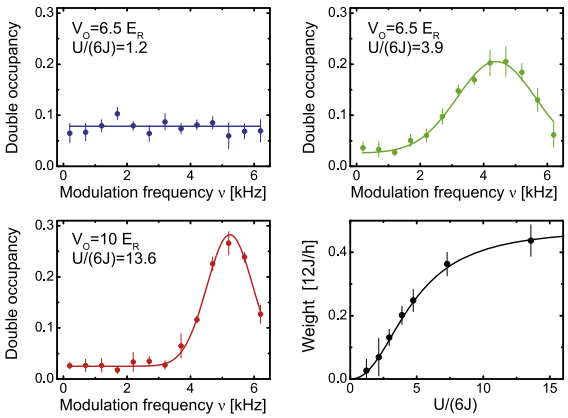

Figure 4. Lattice modulation spectroscopy was used in [106] to verify the existence of a gap, characteristic for the Mott state, for two-component repulsively interacting Fermions in optical lattices. In the Mott state, there is peak in the spectrum whose position and shape depend on the Mott gap given by U. Reproduced with permission from Jördens *et al* [106]. Copyright Macmillan 2008.

10. Static and dynamic structure factors by Bragg spectroscopy

Bragg scattering and spectroscopy have been used as a tool in ultracold gases research since the late 1980s. BECs were for the first time studied by Bragg spectroscopy in [99] and [100]. Bragg spectroscopy provides not only the single particle but also the collective mode spectrum of the gas. This is important concerning both bosonic and fermionic superfluids, and any other many-body states. The dynamic $S(\mathbf{k}, \omega)$ and static $S(\mathbf{k})$ structure factors for Fermi gases were measured with this spectroscopy for the first time by Veeravalli, Vale and coworkers [101].

11. RF, hopping modulation and Bragg spectroscopies in lattices

The use of RF spectroscopy for fermions in the context of optical lattices was pioneered by the group of Esslinger in Moritz *et al* [102] (1D tubes) and in Stöferle *et al* [103] (3D lattices).

Lattice modulation spectroscopy, applicable to both bosons and fermion in lattices, was invented by Esslinger and coworkers in Stöferle *et al* [104] where it was used for

studying the superfluid-Mott insulator transition in a 1D boson gas. In [22] Kollath, Giamarchi and coworkers proposed that this method could be used for fermions as well and theory description of the response in the fermion case was given. For an excellent detailed description of lattice modulation spectroscopy experiments see the book chapter by Tarruell [105].

Breakthroughs observing Mott insulators of fermions in lattices were achieved by Jördens, Esslinger and coworkers [106] and by Schneider, Bloch and coworkers [107]. Lattice modulation spectroscopy was used in [106] to identify the phases, see figure 4. Recently, even short range magnetic correlations have been observed by Greif, Esslinger and coworkers [108], and by Hart, Hulet and coworkers [109]. In [109], spin-sensitive Bragg scattering of light was used to detect the correlations.

12. Universal relations and measuring the contact by the spectroscopies

In ultracold gases, the interparticle interactions have typically a short range but the scattering length is large. Systems with such interactions show universal properties, namely properties that depend on the scattering length only and not on details of the interaction potential. Strong correlations are often resulting from the large scattering lengt. Strongly correlated systems are usually impossible to fully describe with theoretical methods, even non-perturbative ones. Nevertheless, *universal relations* can be derivat that give essential information about the system. An important quantity in the universal relations is so-called *contact*. A lot of universal relations have been found for the two-component interacting Fermi gas. Many universal relations were derived first by Tan [110–112], therefore the name Tan's relations (Tan's contact) that is sometimes used for the universal relations (contact). Derivations that are based on other approaches have been made by Braaten and Platter [113] and by Zhang and Leggett [114]. An excellent in-depth review is given in a book chapter by Braaten [115]. For a reader who wishes a briefer introduction to the topic I recommend section 10.8. of my book chapter [1].

The contact can be defined as [113]

$$C = \int \mathrm{d}^3 R \, \langle \Phi^\dagger \Phi(\mathbf{R}) \rangle . \tag{40}$$

Here g_0 is a coupling constant that depends on the cut-off and $\Phi(\mathbf{R}) = g_0 \psi_2 \psi_1(\mathbf{R})$. Clearly, the contact is very close to the expectation value of the interaction term in the Hamiltonian. It can be understood as a measure of the increased likelihood, due to the strong interactions, of finding two particles close, i.e., closer than the scale of the scattering length, to each other. This means that in the momentum domain, it is a measure of atoms with large momentum. It is usually very difficult to evaluate the contact exactly. Fortunately, it is part of several universal relations which can each be experimentally verified and then compared.

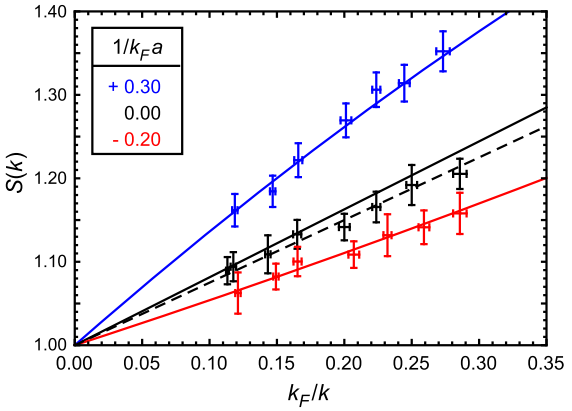

Figure 5. The dependence of the static structure factor $S(k)$ on k_F/k as measured in [117], for different interactions $1/(k_\mathrm{F}a)$. The slope gives the contact according to equation (45) close to unitarity where the second term in the equation is small. Reproduced with permission from Kuhnle *et al* [117]. Copyright APS 2010.

For instance, the adiabatic relation

$$\left(\frac{\mathrm{d}E}{\mathrm{d}a^{-1}}\right)_S = \left(\frac{\mathrm{d}F}{\mathrm{d}a^{-1}}\right)_T = -\frac{\hbar}{4\pi m} C \tag{41}$$

is a thermodynamic relation (including the energy E, the free energy $F = E - TS$ and the entropy S) that connects the contact and the scattering length a.

Also spectroscopies can be used for measuring the contact. The tail of the RF spectrum can be connected to the contact. In a two-component gas with the RF transfer to a third (final) state that does not interact significantly with the two components the result for the tail becomes [116]

$$I(\omega) \to \frac{\Omega^2 \sqrt{\hbar}}{4\pi \sqrt{m}\, \omega^{3/2}} C, \tag{42}$$

where C is the contact between the two species. The scaling of the decay with ω was given in [68] as well, and can be obtained from BCS theory [1]. For RF spectroscopy, there exists a sum rule involving the contact [72, 73]

$$\int_{-\infty}^{\infty} \frac{\mathrm{d}\omega'}{\pi} \omega I(\omega) = \frac{\hbar \Omega^2}{4m} \left(\frac{1}{a_{gg'}} - \frac{1}{a_{ge}} \right) C_{gg'}. \tag{43}$$

The structure factor as well has a tail that gives universal relations. Namely, for the dynamic structure factor

$$S(\omega, k) \to \frac{4q^4}{45\pi^2 \omega (m\omega/\hbar)^{5/2}} \mathcal{C}, \tag{44}$$

and for the static one

$$S(k) \to \frac{1}{8} \left(\frac{1}{k} - \frac{4}{\pi a k^2} \right) \mathcal{C}. \tag{45}$$

Here $\mathcal{C}$ is the contact density which, when integrated over position, gives the contact $C = \int \mathrm{d}^3 r \mathcal{C}(\mathbf{r})$.

Universal relations have been verified in a large number of experiments. Here I mention only some related to

spectroscopies. Kuhnle, Hoinka, Vale and coworkers used Bragg spectroscopy for verifying the universal relation for the tail of the static structure factor as given by equation (45) [117, 118], see figure 5. The contact was obtained by Stewart, Jin and coworkers from a set of universal relations. They measured the tail of the momentum distribution from ballistic expansion and by the momentum-resolved RF spectroscopy (photoemission spectroscopy), and determined the tail of the RF spectrum, equation (42) [119]. These three independent measurements gave values of contact that were in good agreement with each other.

As already discussed, the decaying tail of the RF spectrum is in striking contrast to the superconductor—normal metal experiments where the current continues to grow after the threshold. This is due to momentum conservation in RF spectroscopy. The momentum conservation leads to the fact that the RF spectrum contains information about the spatial correlations, and since the pairing here was based on contact-interaction, the tail reflects the short-range nature of the pairing. This makes intuitive the relation between the tail of the spectrum and the contact.

13. The question of a pseudogap versus a Fermi liquid

One of the outstanding questions that ultracold Fermi gases may give the answer to is the following: what is the nature of the normal state of a strongly interacting Fermi system right above the superfluid critical temperature? Understanding the nature of the normal state is thought to provide a route for discovering even the underlying mechanism of high temperature superconductivity. There are differing theoretical predictions of what the state might be, ranging from a Fermi liquid to the so-called pseudogap state where a gap appears in the single particle excitation spectum already above T_c but corresponds to incoherent Cooper pairs without long-range order. For more information, see for instance various chapters in the book edited by Zwerger [120], such as the one by Strinati [121]. For a description of how pseudogap theories may be probed both in ultracold gases and in cuprates, see the review by Chen, Levin and coworkers [6].

The intriguing situation in the field of ultracold gases is now that there seems to be experimental evidence both for a pseudogap and a Fermi liquid state. Gaebler, Jin, Strinati, and coworkers presented an experiment [122] that combined measurement of the condensate fraction to determine T_c and momentum-resolved RF spectroscopy to measure the single particle spectral function. The observed back-bending of the spectral function around $k = k_F$ matched with a pseudogap theory by Perali, Pieri and Strinati (see also [123]).

Feld, Köhl and coworkers have reported evidence for pseudogap behaviour in *two-dimensional* Fermi gases [124] using momentum-resolved RF spectroscopy (photoemission spectroscopy). Clear shifts of the RF peaks, caused by pairing effects, existed in the spectra well above any superfluid transition. However, the subtle difference between many-body pseudogap and two-body (no Fermi surface needed) pairing in 2D warrants further experimental and theoretical study [13].

All the above reports on pseudogap behaviour were based on photoemission spectroscopy of ^{40}K atoms. On the other hand, Fermi liquid description was found to be sufficient for desribing the strongly interacting normal state in the experiments of Nascimbène, Navon, Jiang, Chevy and Salomon [125, 126] for ^{6}Li atoms. They developed a method to extract the homogeneous equation of state from the density profiles of the trapped gas, which allowed obtaining thermodynamic quantities at high and low temperatures, for balanced and imbalanced gases. Also in the work of Sommer, Zwierlein and coworkers [127] the spin susceptibility of a gas of ^{6}Li was found to agree with a Fermi liquid picture above T_c.

Note that the choice of atom, ^{40}K or ^{6}Li, should not matter even when it seems to do so, because the behaviour of the gas is universal. The apparent differences may better be explained by noting that different atoms allow different probing techniques. For instance the momentum-resolved photoemission spectroscopy is well suited for ^{40}K but not for ^{6}Li. Different probing techniques can emphasize different features of the system.

Recently, Sagi, Jin and coworkers made an interesting experiment [128] with ^{40}K where they removed trapping effects from the momentum-resolved RF spectroscopy response and then modelled it with a simple ansatz that contains a quasiparticle as given by Fermi liquid theory, together with an incoherent background that can describe the physics of pairing:

$$I(k, \omega) = ZI_{\text{coherent}}(k, \omega) + (1 - Z)I_{\text{incoherent}}(k, \omega). \quad (46)$$

The behaviour of the quasiparticle weight Z is expected to depend on temperature [129]. The spectroscopy data was found to match well this description on the BCS side of the crossover and at unitarity, with the quasiparticle weight Z disappearing on the BEC side at $1/(k_F a) = 0.28(0.02)$. Thus Fermi liquid theory seems consistent with the experimental observations until a breakdown point, see figure 6. The article also presents comparisons of the results, for instance the Hartree energy extracted from the data, with quantum Monte-Carlo calculation by Magierski *et al* [77] and crossover theories by Haussmann, Punk and Zwerger [78], Kinnunen [130], and Bruun and Baym [30], with reasonably good match. The work of Haussmann *et al* is based on Luttinger–Ward approach which does not include a pseudogap explicitly; neither does the Brueckner–Goldstone approach by Kinnunen where pairing is not considered but only scattering. On the other hand the work of Bruun and Baym was based on a Nozieres–Schmitt-Rink approach where a pseudogap can be identified.

Incorporating both the superfluid and the normal phase in a sufficiently correct manner to a crossover theory is a formidable theoretical challenge, and even the best crossover theories have their known pitfalls. The experiments have evolved enourmously, nevertheless they still have their limitations in precision and range of parameters that can be explored. Therefore I consider it still an extremely important

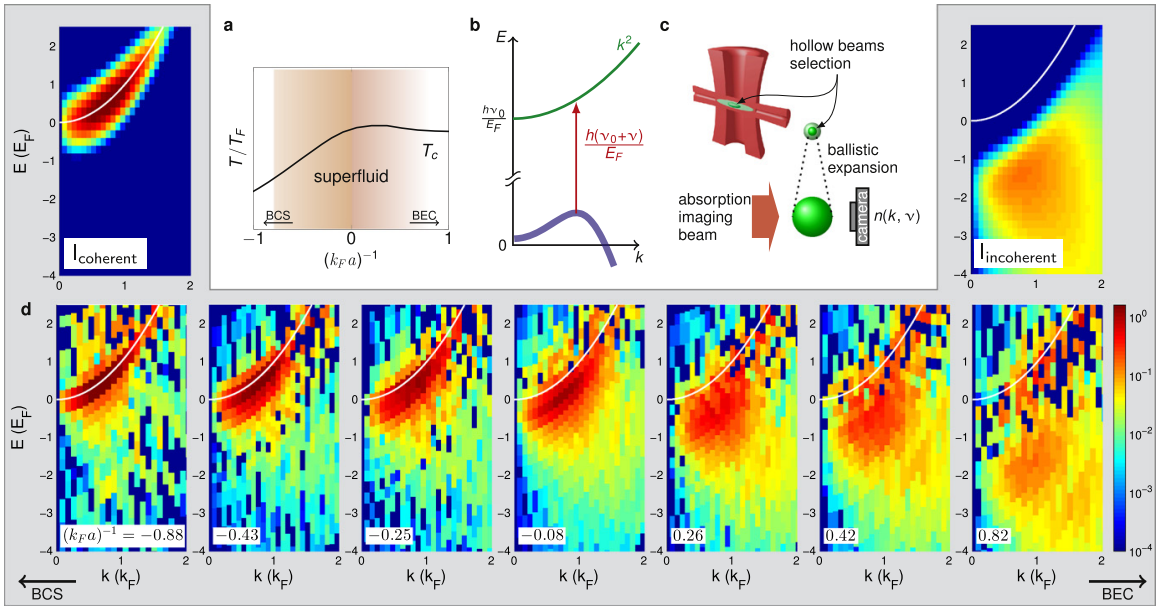

Figure 6. The evolution of momentum-resolved RF spectra (photoemission spectra) throughout the BCS–BEC crossover, from [128]. The evolution is well described by a combination of the coherent part (upper left panel) associated with a quasiparticle weight and an incoherent background (upper right panel). The schematic shows how only the centre of the trap was probed, in order to obtain results that correspond to a homogeneous system. Reproduced with permission from Sagi *et al* [128]. Copyright APS 2015.

future challenge for theory and experiment to nail down the nature of the normal state in a unitary Fermi gas—although at the time of this writing, the Fermi liquid seems to have a slight lead.

14. Outlook

Further experiments and theory on the question whether the strongly interacting normal state is pseudogapped, Fermi liquid, or possibly something else is an obvious important direction of future research. Since the spectral function, gap, and single particle excitations are essential for this question, spectroscopies are likely to turn out to be central in finding the answer.

One-dimensional systems [131] are likely to be an exciting arena to use spectroscopies, not only due to the physics to be expected but because the full field-matter dynamics of a many-body system can be exactly simulated [132, 133]. This allows to study also beyond linear response phenomena.

Concerning many predicted superfluid and strongly correlated states in optical lattices, such as the antiferromagnetic state, the temperatures and entropies have not yet at the time of this writing reached low enough values. Spectroscopies, especially the lattice modulation and Bragg ones, may turn out to play a role in characterizing these states once low enough entropies are reached. The exotic FFLO state is predicted to be stabilized in lattices [134, 135]. In a one-dimensional lattice, it was predicted by exact simulations that the width of the lattice modulation spectra gives direct signatures of the FFLO state [136]. Also RF spectra may show in interesting ways the contributions of the non-paired quasiparticles in the FFLO state [19].

By recent breakthrough experiments [137–140], the field of ultracold gases has entered the rich playground of topologically non-trivial quantum systems. Ultracold gases may be especially suited, for instance, to confirm the recently predicted connection between flat band high-T_c superconductivity and the quantum geometric tensor and the Chern number [141]. How Chern numbers, edge currents, and the like might be characterized by various spectroscopies is a challenge both for theory and experiments. The future of spectroscopies in ultracold Fermi gases seems bright.

Acknowledgments

This work was supported by the Academy of Finland through its Centres of Excellence Programme (2012–2017) and under Project Nos. 263347, 251748, and 272490, and by the European Research Council (ERC-2013-AdG-340748-CODE). Antti Paraoanu is thanked for producing figure 1. The authors of the rest of the figures are thanked for providing the original images and for the kind permission to use them.

References

[1] Törmä P 2015 Spectroscopies—theory *Quantum Gas Experiments—Exploring Many-Body States* ed P Törmä and K Sengstock (London: Imperial College Press) pp 199–250

[2] Bloch I, Dalibard J and Zwerger W 2008 *Rev. Mod. Phys.* **80** 885
[3] Giorgini S, Pitaevskii L and Stringari S 2008 *Rev. Mod. Phys.* **80** 1215–74
[4] Randeria M and Taylor E 2014 *Annu. Rev. Condensed Matter Phys.* **5** 209–32
[5] Ketterle W and Zwierlein M W 2008 Making, probing and understanding ultracold Fermi gases *Proc. Int. School of Phys. 'Enrico Fermi', Course CLXIV (Varenna, Italy, 20–30 June 2006)* ed M Inguscio *et al* (Amsterdam: IOS Press) pp 247–422
[6] Chen Q, He Y, Chien C C and Levin K 2009 *Rep. Prog. Phys.* **72** 122501
[7] Sheehy D E and Radzihovsky L 2007 *Ann. Phys. NY* **322** 1790–924
[8] Radzihovsky L and Sheehy D E 2010 *Rep. Prog. Phys.* **73** 076501
[9] Chevy F and Mora C 2010 *Rep. Prog. Phys.* **73** 112401
[10] Gubbels K and Stoof H 2013 *Phys. Rep.* **525** 255–313
[11] Georges A and Giamarchi T 2010 Strongly correlated bosons and fermions in optical lattices *Many-body Physics with Ultracold Gases: Lecture Notes of the Lex Houches Summer School: Volume 94, July 2010* ed C Salomon, G V Shlyapnikov and L F Cugliandolo (Oxford: Oxford Scholarship Online)
[12] Massignan P, Zaccanti M and Bruun G M 2014 *Rep. Prog. Phys.* **77** 034401
[13] Levinsen J and Parish M 2015 Strongly interacting two-dimensional Fermi gases *Annual Review of Cold Atoms and Molecules: Volume 3* ed K W Madison *et al* (Singapore: World Scientific) pp 1–75
[14] Mahan G 2000 *Many-Particle Physics* 3rd edn (New York: Kluwer Academic, Plenum Publishers)
[15] Grynberg G, Aspect A and Fabre G 2010 *Introduction to Quantum Optics* (Cambridge: Cambridge University Press)
[16] de Gennes P G 1999 *Superconductivity of Metals and Alloys* (Oxford: Westview Press)
[17] Törmä P and Zoller P 2000 *Phys. Rev. Lett.* **85** 487–90
[18] Bruun G M, Törmä P, Rodríguez M and Zoller P 2001 *Phys. Rev.* A **64** 033609
[19] Bakhtiari M R, Leskinen M J and Törmä P 2008 *Phys. Rev. Lett.* **101** 120404
[20] Veillette M, Moon E G, Lamacraft A, Radzihovsky L, Sachdev S and Sheehy D E 2008 *Phys. Rev.* A **78** 033614
[21] Pitaevskii L and Stringari S 2003 *Bose–Einstein Condensation* (Oxford: Oxford University Press)
[22] Kollath C, Iucci A, McCulloch I P and Giamarchi T 2006 *Phys. Rev.* A **74** 041604
[23] Ohashi Y and Griffin A 2005 *Phys. Rev.* A **72** 063606
[24] He Y, Chen Q and Levin K 2005 *Phys. Rev.* A **72** 011602
[25] Kinnunen J, Rodríguez M and Törmä P 2004 *Science* **305** 1131–3
[26] Giaever I 1960 *Phys. Rev. Lett.* **5** 147–8
[27] Minguzzi A, Ferrari G and Castin Y 2001 *Eur. Phys. J.* D **17** 49–55
[28] Rodríguez M and Törmä P 2002 *Phys. Rev.* A **66** 033601
[29] Büchler H P, Zoller P and Zwerger W 2004 *Phys. Rev. Lett.* **93** 080401
[30] Bruun G M and Baym G 2006 *Phys. Rev.* A **74** 033623
[31] Combescot R, Giorgini S and Stringari S 2006 *Europhys. Lett.* **75** 695–701
[32] Challis K J, Ballagh R J and Gardiner C W 2007 *Phys. Rev. Lett.* **98** 093002
[33] Gupta S, Hadzibabic Z, Zwierlein M W, Stan C A, Dieckmann K, Schunck C H, van Kempen E G M, Verhaar B J and Ketterle W 2003 *Science* **300** 1723–6
[34] Regal C A and Jin D S 2003 *Phys. Rev. Lett.* **90** 230404
[35] Zwierlein M W, Hadzibabic Z, Gupta S and Ketterle W 2003 *Phys. Rev. Lett.* **91** 250404
[36] Osheroff D D, Gully W J, Richardson R C and Lee D M 1972 *Phys. Rev. Lett.* **29** 920–3
[37] Leggett A J 1972 *Phys. Rev. Lett.* **29** 1227–30
[38] Houbiers M, Ferwerda R, Stoof H T C, McAlexander W I, Sackett C A and Hulet R G 1997 *Phys. Rev.* A **56** 4864–78
[39] DeMarco B and Jin D S 1999 *Science* **285** 1703–6
[40] Keldysh L 1995 Macroscopic coherent states of excitons in semiconductors *Bose–Einstein Condensation* ed A Griffin *et al* (Cambridge: Cambridge University Press) pp 246–80
[41] Eagles D 1969 *Phys. Rev.* **186** 456
[42] Leggett A 1980 Diatomic molecules and Cooper pairs *Proc. 16th Karpacz Winter School of Theoretical Physics* (Berlin: Springer)
[43] Nozieres P and Schmitt-Rink S 1985 *J. Low Temp. Phys.* **59** 195–393
[44] Parish M M 2015 The BCS–BEC crossover *Quantum Gas Experiments—Exploring Many-Body States* ed P Törmä and K Sengstock (London: Imperial College Press) pp 179–98
[45] Randeria M, Zwerger W and Zwierlein M 2012 *The BCS–BEC Crossover and the Unitary Fermi Gas* ed W Zwerger (Heidelberg: Springer) pp 1–32
[46] Regal C A, Ticknor C, Bohn J L and Jin D S 2003 *Nature* **424** 47
[47] Strecker K, Partridge G and Hulet R 2003 *Phys. Rev. Lett.* **91** 080406
[48] Cubizolles J, Bourdel T, Kokkelmans S J J M F, Shlyapnikov G V and Salomon C 2003 *Phys. Rev. Lett.* **91** 240401
[49] Jochim S, Bartenstein M, Altmeyer A, Hendl G, Chin C, Denschlag J H and Grimm R 2003 *Phys. Rev. Lett.* **91** 240402
[50] Jochim S, Bartenstein M, Altmeyer A, Hendl G, Riedl S, Chin C, Denschlag J H and Grimm R 2003 *Science* **302** 2101–3
[51] Regal C, Greiner M and Jin D 2003 *Nature* **426** 537–40
[52] Zwierlein M W, Stan C A, Schunck C H, Raupach S M F, Gupta S, Hadzibabic Z and Ketterle W 2003 *Phys. Rev. Lett.* **91** 250401
[53] Regal C, Greiner M and Jin D 2004 *Phys. Rev. Lett.* **92** 040403
[54] Zwierlein M W, Stan C A, Schunck C H, Raupach S, Kerman A and Ketterle W 2004 *Phys. Rev. Lett.* **92** 120403
[55] Bartenstein M, Altmeyer A, Riedl S, Jochim S, Chin C, Denschlag J H and Grimm R 2004 *Phys. Rev. Lett.* **92** 203201
[56] Kinast J, Hemmer S L, Gehm M E, Turlapov A and Thomas J E 2004 *Phys. Rev. Lett.* **92** 150402
[57] Bourdel T, Khaykovich L, Cubizolles J, Zhang J, Chevy F, Teichmann M, Tarruell L, Kokkelmans S J J M F and Salomon C 2004 *Phys. Rev. Lett.* **93** 050401
[58] Zwierlein M W, Abo-Shaeer J, Schirotzek A, Schunck C and Ketterle W 2005 *Nature* **435** 1047–51
[59] Zwierlein M W, Schirotzek A, Schunck C H and Ketterle W 2006 *Science* **311** 492–6
[60] Chin C, Bartenstein M, Altmeyer A, Riedl S, Jochim S, Denschlag J H and Grimm R 2004 *Science* **305** 1128–30
[61] Chin C and Julienne P S 2005 *Phys. Rev.* A **71** 012713
[62] Bartenstein M *et al* 2005 *Phys. Rev. Lett.* **94** 103201
[63] Ohashi Y and Griffin A 2005 *Phys. Rev.* A **72** 013601
[64] Shin Y, Schunck C H, Schirotzek A and Ketterle W 2007 *Phys. Rev. Lett.* **99** 090403
[65] Sagi Y, Drake T E, Paudel R and Jin D S 2012 *Phys. Rev. Lett.* **109** 220402
[66] Yu Z and Baym G 2006 *Phys. Rev.* A **73** 063601
[67] Perali A, Pieri P and Strinati G C 2008 *Phys. Rev. Lett.* **100** 010402
[68] Pieri P, Perali A and Strinati G C 2009 *Nat. Phys.* **5** 736

[69] Pieri P, Perali A, Strinati G C, Riedl S, Wright M J, Altmeyer A, Kohstall C, Sánchez Guajardo E R, Hecker Denschlag J and Grimm R 2011 *Phys. Rev.* A **84** 011608
[70] Schunck C H, Shin Y i, Schirotzek A and Ketterle W 2008 *Nature* **454** 739
[71] Schirotzek A, Shin Y i, Schunck C H and Ketterle W 2008 *Phys. Rev. Lett.* **101** 140403
[72] Punk M and Zwerger W 2007 *Phys. Rev. Lett.* **99** 170404
[73] Baym G, Pethick C J, Yu Z and Zwierlein M W 2007 *Phys. Rev. Lett.* **99** 190407
[74] Basu S and Mueller E J 2008 *Phys. Rev. Lett.* **101** 060405
[75] Stewart J, Gaebler J and Jin D 2008 *Nature* **454** 744
[76] Kinnunen J, Rodríguez M and Törmä P 2004 *Phys. Rev. Lett.* **92** 230403
[77] Magierski P, Wlazlowski G, Bulgac A and Drut J E 2009 *Phys. Rev. Lett.* **103** 210403
[78] Haussmann R, Punk M and Zwerger W 2009 *Phys. Rev.* A **80** 063612
[79] Shin Y, Zwierlein M W, Schunck C H, Schirotzek A and Ketterle W 2006 *Phys. Rev. Lett.* **97** 030401
[80] Partridge G B, Li W, Kamar R I, Liao Y A and Hulet R G 2006 *Science* **311** 503–5
[81] Chandrasekhar B S 1962 *Appl. Phys. Lett.* **1** 7–8
[82] Clogston A M 1962 *Phys. Rev. Lett.* **9** 266–7
[83] Nascimbène S, Navon N, Jiang K J, Tarruell L, Teichmann M, McKeever J, Chevy F and Salomon C 2009 *Phys. Rev. Lett.* **103** 170402
[84] Lobo C, Recati A, Giorgini S and Stringari S 2006 *Phys. Rev. Lett.* **97** 200403
[85] Kim D H, Kinnunen J J, Martikainen J P and Törmä P 2011 *Phys. Rev. Lett.* **106** 095301
[86] Parish M M and Huse D A 2009 *Phys. Rev.* A **80** 063605
[87] Liao Y A, Revelle M, Paprotta T, Rittner A S C, Li W, Partridge G B and Hulet R G 2011 *Phys. Rev. Lett.* **107** 145305
[88] Shin Y, Schunck C H, Schirotzek A and Ketterle W 2008 *Nature* **451** 689
[89] Parish M M, Marchetti F M, Lamacraft A and Simons B D 2007 *Nat. Phys.* **3** 124–8
[90] Haussmann R, Rantner W, Cerrito S and Zwerger W 2007 *Phys. Rev.* A **75** 023610
[91] Carlson J and Reddy S 2008 *Phys. Rev. Lett.* **100** 150403
[92] Schirotzek A, Wu C H, Sommer A and Zwierlein M W 2009 *Phys. Rev. Lett.* **102** 230402
[93] Kohstall C, Zaccanti M, Jag M, Trenkwalder A, Massignan P, Bruun G M, Schreck F and Grimm R 2012 *Nature* **485** 615
[94] Koschorreck M, Pertot D, Vogt E, Frohlich B, Feld M and Köhl M 2012 *Nature* **485** 619
[95] Fröhlich B, Feld M, Vogt E, Koschorreck M, Zwerger W and Köhl M 2011 *Phys. Rev. Lett.* **106** 105301
[96] Sommer A T, Cheuk L W, Ku M J H, Bakr W S and Zwierlein M W 2012 *Phys. Rev. Lett.* **108** 045302
[97] Zhang Y, Ong W, Arakelyan I and Thomas J E 2012 *Phys. Rev. Lett.* **108** 235302
[98] Murthy P A, Boettcher I, Bayha L, Holzmann M, Kedar D, Neidig M, Ries M G, Wenz A N, Zürn G and Jochim S 2015 *Phys. Rev. Lett.* **115** 010401
[99] Kozuma M, Deng L, Hagley E W, Wen J, Lutwak R, Helmerson K, Rolston S L and Phillips W D 1999 *Phys. Rev. Lett.* **82** 871–5
[100] Stenger J, Inouye S, Chikkatur A P, Stamper-Kurn D M, Pritchard D E and Ketterle W 1999 *Phys. Rev. Lett.* **82** 4569–73
[101] Veeravalli G, Kuhnle E, Dyke P and Vale C J 2008 *Phys. Rev. Lett.* **101** 250403
[102] Moritz H, Stöferle T, Günter K, Köhl M and Esslinger T 2005 *Phys. Rev. Lett.* **94** 210401
[103] Stöferle T, Moritz H, Günter K, Köhl M and Esslinger T 2006 *Phys. Rev. Lett.* **96** 030401
[104] Stöferle T, Moritz H, Schori C, Köhl M and Esslinger T 2004 *Phys. Rev. Lett.* **92** 130403
[105] Tarruell L 2015 Spectroscopic tools for experiments with ultracold fermions in optical lattices *Quantum Gas Experiments—Exploring Many-Body States* ed P Törmä and K Sengstock (London: Imperial College Press) pp 251–66
[106] Jördens R, Strohmaier N, Günter K, Moritz H and Esslinger T 2008 *Nature* **455** 204
[107] Schneider U, Hackermuller L, Will S, Best T, Bloch I, Costi T A, Helmes R W, Rasch D and Rosch A 2008 *Science* **322** 1520
[108] Greif D, Uehlinger T, Jotzu G, Tarruell L and Esslinger T 2013 *Science* **340** 1307
[109] Hart R A, Duarte P M, Yang T L, Liu X, Paiva T, Khatami E, Scalettar R T, Trivedi N, Huse D A and Hulet R G 2015 *Nature* **519** 211–4
[110] Tan S 2008 *Ann. Phys. NY* **323** 2952–70
[111] Tan S 2008 *Ann. Phys. NY* **323** 2971–86
[112] Tan S 2008 *Ann. Phys. NY* **323** 2987–90
[113] Braaten E and Platter L 2008 *Phys. Rev. Lett.* **100** 205301
[114] Zhang S and Leggett A J 2009 *Phys. Rev.* A **79** 023601
[115] Braaten E 2012 Universal relations for fermions with large scattering lengths *The BCS–BEC Crossover and the Unitary Fermi Gas* ed W Zwerger (Heidelberg: Springer) pp 193–231
[116] Schneider W and Randeria M 2010 *Phys. Rev.* A **81** 021601
[117] Kuhnle E D, Hu H, Liu X J, Dyke P, Mark M, Drummond P D, Hannaford P and Vale C J 2010 *Phys. Rev. Lett.* **105** 070402
[118] Hoinka S, Lingham M, Fenech K, Hu H, Vale C J, Drut J E and Gandolfi S 2013 *Phys. Rev. Lett.* **110** 055305
[119] Stewart J T, Gaebler J P, Drake T E and Jin D S 2010 *Phys. Rev. Lett.* **104** 235301
[120] Zwerger W 2012 *The BCS–BEC Crossover and the Unitary Gas* (Berlin: Springer)
[121] Strinati G 2012 Pairing fluctuations approach to the BCS–BEC crossover *The BCS–BEC Crossover and the Unitary Fermi Gas* ed W Zwerger (Heidelberg: Springer) pp 99–126
[122] Gaebler J P, Stewart J T, Drake T E, Jin D S, Perali A, Pieri P and Strinati G C 2010 *Nat. Phys.* **6** 569
[123] Perali A, Palestini F, Pieri P, Strinati G C, Stewart J T, Gaebler J P, Drake T E and Jin D S 2011 *Phys. Rev. Lett.* **106** 060402
[124] Feld M, Fröhlich B, Vogt E, Koschorreck M and Köhl M 2011 *Nature* **480** 75
[125] Nascimbène S, Navon N, Jiang K J, Chevy F and Salomon C 2010 *Nature* **463** 1057
[126] Navon N, Nascimbène S, Chevy F and Salomon C 2010 *Science* **328** 729
[127] Sommer A, Ku M, Roati G and Zwierlein M 2011 *Nature* **472** 201
[128] Sagi Y, Drake T E, Paudel R, Chapurin R and Jin D S 2015 *Phys. Rev. Lett.* **114** 075301
[129] Doggen E V H and Kinnunen J J 2015 *Sci. Rep.* **5** 9539
[130] Kinnunen J J 2012 *Phys. Rev.* A **85** 012701
[131] Giamarchi T 2007 *Quantum Physics in One Dimension* (Oxford: Oxford University Press)
[132] Daley A, Kollath C, Schollwöck U and Vidal G 2004 *J. Stat. Mech.* P04005
[133] Leskinen M J, Nummi O H T, Massel F and Törmä P 2010 *New J. Phys.* **12** 073044
[134] Koponen T K, Paananen T, Martikainen J P and Törmä P 2007 *Phys. Rev. Lett.* **99** 120403
[135] Heikkinen M O J, Kim D H, Troyer M and Törmä P 2014 *Phys. Rev. Lett.* **113** 185301

[136] Korolyuk A, Massel F and Törmä P 2010 *Phys. Rev. Lett.* **104** 236402
[137] Aidelsburger M, Atala M, Lohse M, Barreiro J T, Paredes B and Bloch I 2013 *Phys. Rev. Lett.* **111** 185301
[138] Miyake H, Siviloglou G A, Kennedy C J, Burton W C and Ketterle W 2013 *Phys. Rev. Lett.* **111** 185302
[139] Jotzu G, Messer M, Desbuquois R, Lebrat M, Uehlinger T, Greif D and Esslinger T 2014 *Nature* **515** 237
[140] Aidelsburger M, Lohse M, Schweizer C, Atala M, Barreiro J T, Nascimbène S, Cooper N, Bloch I and Goldman N 2015 *Nat. Phys.* **11** 162–6
[141] Peotta S and Törmä P 2015 *Nat. Commun.* **6** 8944